INVESTIGATION OF POLYVINYL ALCOHOL (PVOH) ADDED KENAF NANOWHISKER AND MONTMORILLONITE (MMT)

MAH BEE LING

A project report submitted in partial fulfilment of the requirements for the award of Bachelor of Engineering (Hons.) Chemical Engineering

Lee Kong Chian Faculty of Engineering and Science
Universiti Tunku Abdul Rahman

April 2015

DECLARATION

I hereby declare that this project report is based on my original work except for citations and quotations which have been duly acknowledged. I also declare that it has not been previously and concurrently submitted for any other degree or award at UTAR or other institutions.

Signature : _____

Name : MAH BEE LING

ID No. : 10UEB03504

Date : _____

APPROVAL FOR SUBMISSION

I certify that this project report entitled **"INVESTIGATION OF POLYVINYL ALCOHOL (PVOH) ADDED KENAF NANOWHISKER AND MONTMORILLONITE (MMT)"** was prepared by **MAH BEE LING** has met the required standard for submission in partial fulfilment of the requirements for the award of Bachelor of Engineering (Hons.) Chemical Engineering at Universiti Tunku Abdul Rahman.

Approved by,

Signature : _____

Supervisor : Ir. Prof. Dr. Tee Tiam Ting

Date : _____

Specially dedicated to
my beloved mother, brother and sister

ACKNOWLEDGEMENTS

I would like to thank everyone who had contributed to the successful completion of this project. I would like to express my gratitude to my research supervisor, Ir. Prof. Dr. Tee Tiam Ting for his invaluable advice, guidance and his enormous patience throughout the development of the research. Besides, I would also like to thank Ir. Dr. Lee Tin Sin and Dr. Bee Soo Tueen for their initiative to guide me throughout this research.

In addition, I would also like to express my gratitude to my loving parent and friends who had helped and given me encouragement in terms of moral and financial in completing this research successfully.

INVESTIGATION OF POLYVINYL ALCOHOL (PVOH) ADDED KENAF NANOWHISKER AND MONTMORILLONITE (MMT)

ABSTRACT

In this study, the nanocomposites made of polyvinyl alcohol (PVOH), kenaf nanowhisker and montmorillonite (MMT) were prepared and analysed. Kenaf nanowhisker loading was varied from 0 phr to 8 phr while MMT loading was varied from 1 phr to 5 phr. In overall, the tensile strength exhibited highest value at 5 phr of MMT and modulus exhibited the highest value at 3 phr of MMT loading although increasing MMT loading could reduce the elongation at break. Increment of kenaf nanowhisker loading would increase the tensile strength, elongation and modulus until a maximum point followed by dropping of the mechanical properties. Among all, nanocomposite with 5 phr of MMT with no addition of kenaf nanowhisker has the highest tensile strength. Differential scanning calorimetry (DSC) results showed that the peak heating temperature of amorphous region was highest at 141.39°C when 5 phr of MMT was incorporated into PVOH without addition of kenaf nanowhisker. This showed that MMT has good interaction with PVOH whereas kenaf nanowhisker provides lesser reinforcing effect. Scanning electron microscopy (SEM) images supported that increasing kenaf nanowhisker and MMT loading could induce agglomeration and formation of flakes-like structure. At low kenaf nanowhisker loading, PVOH matrix showed high continuity which contributed to high tensile strength. Addition of kenaf nanowhisker beyond maximum loading could decrease the tensile strength attributed by formation of agglomeration. XRD showed that a new peak was formed at $2\theta = 22°$ with the incorporation of kenaf nanowhisker and MMT into PVOH. At high kenaf nanowhisker loading, crystallinity increased with increasing amount of MMT.

TABLE OF CONTENTS

LIST OF TABLES

LIST OF FIGURES

LIST OF SYMBOLS / ABBREVIATIONS

mL	millilitre
phr	Part per hundred resin
rpm	Revolutions per minute
T_g	Glass transition temperature, °C
T_m	Melting temperature, °C
DSC	Differential scanning calorimetry
FTIR	Fourier transform and infrared
H_2SO_4	Sulphuric acid
MMT	Montmorillonite
$NaClO_2$	Sodium chlorite
NaOH	Sodium hydroxide
PVOH/PVA	Poly (vinyl alcohol)
SEM	Scanning electron microscopy
TGA	Thermogravimetric analysis
XRD	X-ray diffraction

CHAPTER 1

INTRODUCTION

1.1 Background

Over the past decades, biodegradable polymer, especially in packaging applications, has gradually become concern of researcher groups to develop environmental friendly materials. Many researches and studies have been carried out to develop new material which has low impact to environment (Kowalczyk, et al., 2011). Due to over consuming, price of those environmental friendly biopolymers rising making them become expensive. Therefore, polymers are compounded with other natural materials such as starch and cellulose fibres to reduce cost while maintain or enhancing the mechanical and thermal properties.

Polyvinyl alcohol (PVOH) which sometimes known as PVA is one of the biodegradable synthetic polymers derived from petroleum (Chen, et al., 1999). It is a water-soluble hydrophilic polymer produced by hydrolysis of poly vinyl acetate with alternating secondary hydroxyl (–OH) groups. (Marten and Zvanut, 1992). PVOH has high degree of crystallinity due to the small sized hydroxyl group able to suit into the crystal structure forming highly orientated structure (Bee, et al., 2014). PVOH is biodegradable as it can be consumed by more than 20 types of microorganisms such as yeasts, bacteria and molds and their enzymes naturally (Reho, 2012).

Due to the wide application of PVOH, the price of PVOH is increasing and become expensive to use PVOH as raw material in industrial, packaging, medical and other applications. Besides that, extensive application of PVOH requires it to

provide better mechanical properties and thermal characteristics to fulfil the increasing requirements. Composite is produced by dispersing of foreign particles into a polymer matrix to achieve improved properties. Thus, many low-cost materials have been introduced to compound with PVOH to minimize the production cost while improve its mechanical properties. Natural fibers have become a new concern by researchers and manufacturers in composite applications. Utilization of natural fibers exhibit many preferences compared to synthetic fibers, for example low tool wear (Wambua, Ivens and Verpoest, 2003), biodegradability, lower cost, available in abundant and low density (Nishino, et al., 2003). One of the new natural materials that have the potential for use in composite polymer is kenaf cellulose fibres.

Since kenaf is able to grow in a short period under a variety of weather conditions, it is well known to have economic and ecological advantage (Aziz, et al., 2005). Kenaf is a kind of plant and member of hibiscus family. Its main producer countries are Asian countries (Gilberto, Bras and Alain, 2010). It is a natural renewable resource with high growth rate and available in abundant. Due to kenaf has high cellulose content (Shi, et al., 2011) but low cost, it act as a good reinforcement compound to produce polymer composite with lower cost and enhanced properties. Many researches have been carried out to determine the compatibility of kenaf fibre with various polymers such as PVOH, polylactic acid, polypropylene, maleic anhydride-grafted polypropylene (Nina, et al., 2014; Fortunati, et al., 2014). Properties of fibre-reinforced composites are significantly influenced by interaction between each other.

The use of nano-sized fibres increases the interface area between fibre and polymer matrix and thus promoting good interaction. According to Zadorecki and Anthony (1989), crystallite has highest elastic modulus compared to solid wood, single pulp fibre and microfibrils. Thus, the strength of the fibres can be increased by breaking down the cellulosic fibre into nanoscale. Shi, et al. (2011) found out that PVOH-kenaf nanowhisker composite has remarkable enhanced tensile strength of 46.2% compared to virgin PVOH when only 9 wt% of kenaf nanowhisker are added. Both PVOH and kenaf nanowhisker has hydroxyl groups. Based on the research (Shi, et al., 2011), the improved strength may be due to the hydrogen bond formed between kenaf nanowhisker and PVOH.

Montmorillonite (MMT) is the most common smectite group mineral used as reinforcing inorganic filler in polymer-silicate nanocomposites to improve properties of virgin polymer or composite polymer (Tee, et al., 2012). MMT has a crystal layered structure with 1 nm layers with a central octahedral sheet of alumina attached between two external silica tetrahedral sheets where the oxygen from the tetrahedral sheet also belongs to the silica tetrahedral. MMT is chemically and physically stable. It has high aspect ratio and large volume fraction which may contribute to better mechanical, thermal and physical properties. (Lakshmi, Narmadha and Reddy, 2007). MMT is hydrophilic due to presence of sodium cation between the interlayer (Majdzadeh-Ardakani and Nazari, 2010). Thus, MMT is miscible with water-soluble hydrophilic polymer such as PVOH.

Strawhecker and Mannias (2000) found out that the mechanical and thermal properties of virgin PVOH increased when MMT is added into PVOH at certain composition. Therefore, MMT is expected to have good miscibility and compatibility with PVOH-kenaf nanowhisker composite and therefore enhance its mechanical and thermal properties. However, the improvement depends not only on the compatibility between polymer matrix and MMT, but also dependent on concentration of MMT incorporated.

1.2 Problem Statements

Current trends in plastic industry wanting polymer which are renewable, biodegradable, environment friendly and non-toxic (Tang and Alavi, 2011). Kenaf cellulose fibre is one which fulfils the requirements above. Thus, kenaf is often blending with other polymer to produce nanocomposite with enhanced mechanical and thermal properties. PVOH is used in wide range of industrial field due to its biodegradable and excellent properties. However, the price of PVOH is hiking making it become an expensive polymer. To reduce the cost, PVOH is mixed with other compound which is compatible, such as kenaf nano whisker. Nano-sized filler, montmorillonite (MMT) is added to stabilize the PVOH-kenaf nanowhisker blend and further improve the mechanical properties. Hence, this study is to evaluate the

effect of MMT added to PVOH-kenaf nanowhisker blend. Following are the problem statements:

1. What are the mechanical and thermal properties as MMT is added into PVOH-kenaf nanowhisker blends?
2. What are the microstructures and interactions between the blended compounds when PVOH is mixed with kenaf nanowhisker and MMT?

1.3 Objectives

The objective of this study was to understand the key interactions between PVOH, kenaf nanowhisker and MMT and also investigate the optimum combination of kenaf nanowhisker and MMT added to PVOH. To achieve the main objective, few sub-objectives are identified as below:

1. To evaluate the mechanical and thermal properties of PVOH-kenaf nanowhisker- MMT blends.
2. To analyze the microstructure between each blended compounds.

1.4 Scopes of Study

This study was focusing on preparation and characterization of PVOH- kenaf nanowhisker- MMT blends. Blends of PVOH, kenaf and MMT were prepared at different composition. The samples were compounded using casting method and then cut into dumbbell shape and rectangular shape. Several techniques and tests were carried out to characterise the blend of MMT with PVOH-kenaf nanowhisker as below:

1.4.1 Mechanical properties

Tensile test was carried out to determine the tensile strength, Young's modulus and elongation at break. This test was performed according to ASTM D 882 standard.

1.4.2 Thermal properties (DSC)

The onset and endpoint melting temperature of the PVOH- kenaf nanowhisker- MMT blends were obtained from Differential Scanning Calorimetry (DSC) test.

1.4.3 Microstructure (SEM and XRD)

Scanning Electron Microscopy (SEM) was carried out to determine the microstructure of PVOH- kenaf nanowhisker- MMT blends. X-ray Diffraction (XRD) will be used to analyse the crystallinity and dispersion of kenaf nanowhisker and MMT in the PVOH matrix.

CHAPTER 2

LITERATURE REVIEW

2.1 Polyvinyl alcohol (PVOH)

Polyvinyl alcohol (PVOH) is a polymer of vinyl alcohol. It is odourless and does not release dangerous vapour. It has simple chemical structure with hydroxyl pendant group as shown in Figure 2.1 below. PVOH is a water-soluble semi-crystalline polymer. For fully hydrolysed PVOH, it is not a thermoplastic as its meting point temperature is higher than its degradation temperature. PVOH is not prepared directly from its monomer, vinyl alcohol as it is unstable to acetaldehyde. PVOH is prepared by hydrolysis of polyvinyl acetate through polymerization of vinyl acetate (Olabisi, 1997).

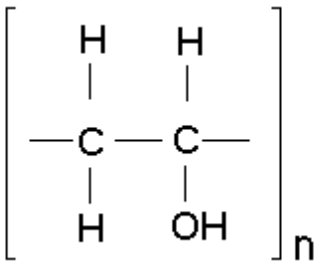

Figure 2.1: Structure of Polyvinyl Alcohol (PVOH)

PVOH has high tensile strength, flexibility, strong and durable. However, the mechanical properties, crystallinity, solubility (Finch, 1973) and its specific functional uses depend on the degree of hydrolysis, degree of polymerization and

molecular weight. Generally, PVOH is categorized into two classes, namely fully hydrolysed and partially hydrolysed. PVOH with high degree of hydrolysis is less soluble in water compared to PVOH with low degree of hydrolysis (Hassan and Peppas, 2000). The fully hydrolyzed PVOH is commonly has higher crystallinity than partially hydrolyzed PVOH (Bee, et al., 2014). Therefore, fully hydrolysed PVOH is more preferable in industries as it has stronger intermolecular hydrogen bonds that linked the chains together and thus exhibits stronger mechanical properties (Rwei and Huang, 2012). These strong hydrogen bonds inhibit the motion of the chains within the matrix, contributing to higher strength and rigidity.

PVOH can be considered as a good host matrix due to chemical resistance, good thermo-stability and film forming ability (Guirguis and Moselhey, 2011). It is also non-toxic and resistant to solvent, oil and grease. PVOH can be processed by solution casting and form PVOH films as it is soluble in water. Therefore, PVOH is widely used in industrial, as packaging films, textile sizing agent, paper adhesives and paper coatings (Chang, et et., 2003). However, PVOH is an expensive material. To reduce cost of production, PVOH is usually mixed with other low cost fillers such as starch or natural fibers with acceptable enhancement reduction of mechanical properties.

2.2 Types of additives

Typically, commercial plastics are mixture of polymers and additives. Virgin polymers may not provide the various requirements of final product such as good mechanical properties, resistant to thermal degradation, outstanding appearance etc. Therefore, additives are normally incorporated into virgin polymers. The main reason for using additives are property modification or enhancement, cost reduction and improving processability characteristics.

Different types of additives may provide different property required. Examples of few common additives used for polymers include fillers, reinforcements, plasticizers, thermal and light stabilizers, impact modifiers, flame-retardant agents,

colorants, processing aids, blowing agent and biocides (Fried, 1995). Table 2.1 below shows the effects of different additives on polymer properties.

Table 2.1: Effects of Additives on Polymer Properties (Dc.engr.scu.edu, 2014)

Additives	Common materials	Effects of polymer properties
Reinforcing fibers	Baron, carbon, fibrous minerals, glass, Kevlar	• Increase tensile strength. • Increase flexural modulus. • Increase heat-deflection temperature (HDT). • Resist shrinkage and warpage.
Conductive fillers	Aluminium powders, carbon fiber, graphite	• Improves electrical and thermal conductivity.
Coupling agents	Silanes, titanates	• Improve interface bonding between polymer matrix and fibers.
Flame retardants	Chlorine, bromine, phosphorus, metallic salts	• Reduce the occurrence and spread of combustion.
Extender fillers	Calcium carbonate, silica, clay	• Reduces material cost.
Plasticizers	Monomeric liquids, low-molecular weight materials	• Improves melt flow properties. • Enhances flexibility.
Colorants (pigments and dyes)	Metal oxides, chromates, carbon blacks	• Provide colourfastness. • Protects from thermal and UV degradation (with carbon blacks).
Blowing agents	Gas, azo compounds, hydrazine derivatives	• Generate a cellular form to obtain a low-density material.

2.3 Kenaf cellulose fibers

2.3.1 Cellulose

Main function of fillers for thermoplastics and thermosets is to reduce overall production cost. Some filler may also acts to modify the properties of polymer. For example, carbon black can be used to minimize electrical charging while mica is used to modify the heat-insulating properties (Fried, 1995).

As environmental friendly materials are now becoming concern in polymer field, renewable and sustainable cellulose had increasing demand as fillers. The cellulose fiber reinforcement produced from biological plant cell wall show high mechanical properties (Wang, 2011). Besides, a fast development of polymer nanocomposites, which are polymers compounded with spheres, fibers, or plates with dimension below 100 nm also leads to research interest in nanosized cellulose (Wang, 2011). Natural cellulose exists as highly-ordered microfibrils with nanoscale and is expected to be stiffer than many synthetic fibers (Wang, 2011). The nanoscopic nature of the filler contribute to the large relative surface area and hence exhibits unique mechanical, thermal, electrical, and optical properties of the composites, providing opportunities to produce light-weight structural materials as well as advanced biomedical and electronic devices (Wang, 2011). Basically, there are two family of cellulose nanofiller, name as cellulose nanocrystals and microfibrillated cellulose (Siqueira, Bras and Dufresne, 2010). Both cellulose nanocrystals and microfibrillated cellulose have at least one-dimension in nanoscale that is 1-100nm although microfibrillated cellulose has the term “micro”. Cellulose nanocrystals are also known as nanowhisker. The difference between cellulose nanocrystals and microfibrillated cellulose is that cellulose nanocrystals are products from extraction of cellulose from the plant cell wall by process called chemical hydrolysis whereas microfibrillated cellulose is extracted through mechanical homogenization treatment.

The plant cell wall exhibits good mechanical properties which give cells rigidity, strength and flexibility, which are preferred in manufacture of polymer products (Wang, 2011). The good mechanical properties are due to the presence of crystalline cellulose and the hierarchical structure. There are three main components

make up the natural fibers, which include hemicellulose, cellulose and lignin. In another word, stiff cellulose microfibrils are surrounded by a matrix composed of hemicellulose and lignin which make up an individual fiber (Siqueira, Bras and Dufresne, 2010). Cellulose crystallites provide the high stiffness and mechanical properties of the fibers by forming hydrogen bonds and other bonds, hemicellulose is in control for thermal degradation, moisture absorption and biodegradation while lignin is responsible for the decomposition of the fibers by ultraviolet (UV) (Akil, et al., 2011). There are many factors, for examples internal fiber structure, chemical composition, cell dimensions, imperfections and microfibril angle, that influence the properties of cellulose fibers (Dufresne, 2008). Besides, the cellulose type will also highly affect the mechanical properties of natural fibers because different crystalline organization will gives different mechanical properties (Bledzki and Gassan, 1999).

Cellulose is a linear homopolysaccharide made up of β-glucopyranose units bonded together by β-1-4-linkages (Brännvall, 2007). Figure 2.2 below shows the basic structure of cellulose. Each monomer has three hydroxyl groups. These hydroxyl groups can form hydrogen bonds and therefore contribute to crystalline order and also controlling the physical properties of cellulose (John and Thomas, 2008).

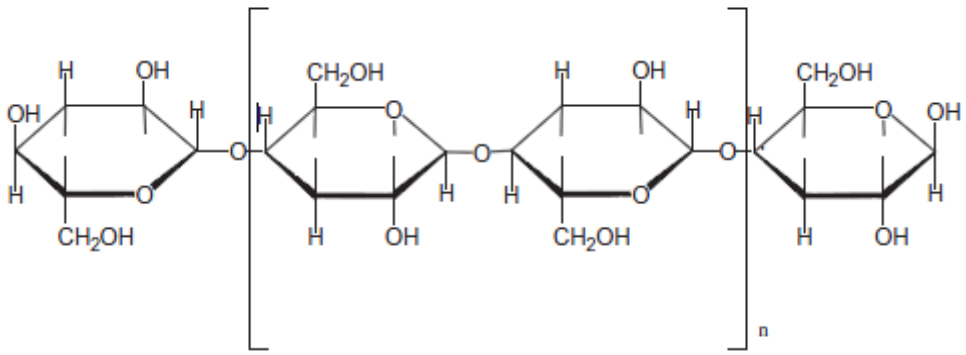

Figure 2.2: Basic Chemical Structure of Cellulose (Akil et. al., 2011)

Cellulose is made by cellulose microfibril during biosynthesis as shown in Figure 2.3. The fibril, which is a long string-like bundle of molecules is formed by aggregation of poly-β-(1→4)-D-glucosyl and linked by intermolecular hydrogen bonds (Andresen et. al., 2006). Cellulose microfibrils have both crystalline regions and

amorphous regions. Single cellulose microfibril have diameters in the range of 2 nm to 20 nm and consists of a thread of cellulose crystals bonded along the microfibril axis by disordered amorphous regions (Azizi Samir, Alloin and Dufresne, 2005). Amorphous has lower degree of order and thus is not preferable.

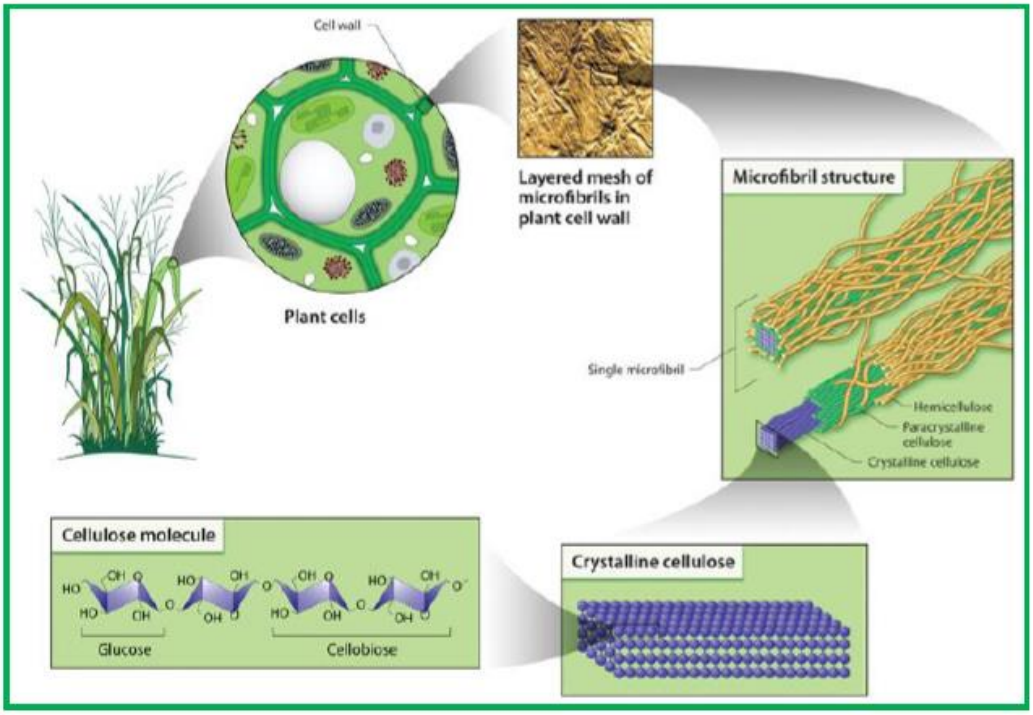

Figure 2.3: Extraction of Microfibrils from Cellulose Cell Wall (Siqueira, Bras and Dufresne, 2010)

Native cellulose, also known as cellulose I is the crystalline cellulose. Cellulose nanofillers are produced from extraction of the native cellulose (cellulose I) by conventional bleaching treatments of lignocellulosic fibers. High modulus, low density and high crystallinity of Cellulose I make it a good alternative to conventional reinforcements such as glass fibers and carbon fibers.

2.3.2 Kenaf nanowhisker

Recently, kenaf has been found to be a new and significant source of natural fiber for composites. Nishino, et al., (2003) found out that kenaf is biodegradable, resistant to abrasive during processing, low density and has good mechanical properties in specific applications.

Kenaf is known as dicotyledonous plant as the stalk has three layers. The inner layer core called xylem. The outer layer bark called phloem. Whereas pith is the central thin layer which comprise of soft tissue with mostly non-ferrous cells (Ashori, et al., 2006). Kenaf bast occupied one-third of the plant and is reported that it has higher mechanical properties than other parts of the plant (Aji, et al., 2009). Kenaf nanowhisker is extracted through sulphuric acid hydrolysis. Nanowhisker is more preferable than microfibrillated cellulose due to nanowhisker only contains crystallites whereas microfibrillated cellulose contains both crystallites and disordered amorphous regions. Microfibrillated is also not preferred because during production of microfibrillated cellulose is that the energy consumption during the homogenization process and pre-treatment such as acid hydrolysis and enzymatic hydrolysis are needed to solve this problem (Siqueira, Bras and Dufresne, 2010). Furthermore, Lu, Wang and Drzal in their research reported that the reinforcing effect of microfibrillated cellulose is not as efficient as nanowhisker, although microfibrillated cellulose has easier preparation method.

Araki, et al. (2001) had done a study to compare the difference hydrochloric acid and sulphuric acid used to isolate cellulose nanocrystals. They found out that sulphuric acid can provide more stable aqueous suspensions than hydrochloric acid.

2.3.3 Kenaf nanowhisker as nanocomposites

The incorporation of kenaf nanowhisker is only applicable and limited to polar polymer because of their polar surface. Therefore, water-soluble polymers such as polyvinyl alcohol (PVOH) and polyoxyethylene (POE) are mainly used as the

hydrophilic kenaf nanowhisker can have good dispersion and adhesion into the polymer matrix. However in non-polar medium, the kenaf nanowhisker cannot distribute well in it due to its hydrophilic character. There are two main techniques used to prepare cellulose nanocomposite films (Dufresne, n.d.), which are organic or water solvent evaporation by solvent casting and extrusion with freeze-dried cellulose nanoparticles.

The first technique to get cellulose reinforced nanocomposites is the most commonly used where the polymer nanocomposite is prepared by mixing the nanoparticle suspensions in an organic medium with a polymer solution. The second method is the extrusion method with melting compounding technique. In this method, the main problem encountered is the cellulose nanoparticles are in the dry state. Certainly, as these polysaccharides nanoparticles are dried, strong intermolecular hydrogen bonds form and aggregates are obtained limiting the nanosized reinforcement. Helbert, et al. (1996) illustrated that nanocomposites prepared by casting and evaporating exhibit higher mechanical properties than nanocomposites prepared by freeze-drying and hot-pressing. High cost of freeze-drying also makes them economically unfavourable.

2.4 Montmorillonite (MMT)

Inorganic additives are one of the reinforcements to enhance the physical properties and resist deformation of thermoplastics. There are many types of inorganic reinforcements, generally classified as natural minerals and synthetic minerals. They are able to form a network of restraining points in the polymer whereby the polymer is restricted to motion. Silicate is one of the most interesting class of minerals. Silicates exhibits high tensile strength, high modulus and heat resistance (Visakh, et al., 2013). The silicates are grouped according to their structure, namely phyllosilicates, cyclosilicates, nesosilicates, sorosilicates, tectosilicates and inosilicates. Layered silicates are belongs to physillosilicate. Among layered silicates, smectite group with 2:1 type are the most important reinforcement fillers in polymers.

Montmorillonite (MMT) is silicate clay minerals. It is one of the natural phyllosilicate smectite with 2:1 ratio, which means it has two tetrahedral sheets with a central octahedral sheet. The formula for MMT is $[(Na,Ca)_{0.33}(Al, Mg)_2(Si_4O_{10})(OH)_2\text{-}nH_2O]$. Figure 2.4 below shows the structure of MMT. MMT is known as smectite because of its ability to absorb water due to large spacing and weak bonding between layered sheets. In nature, MMT is hydrophilic due to the presence of cations within the crystalline layers (He, et al., 2008). The hydrophilic character besides enable inorganic crystalline layers of MMT to form suspension in water, also promote dispersion in water-soluble polymers such as PVOH.

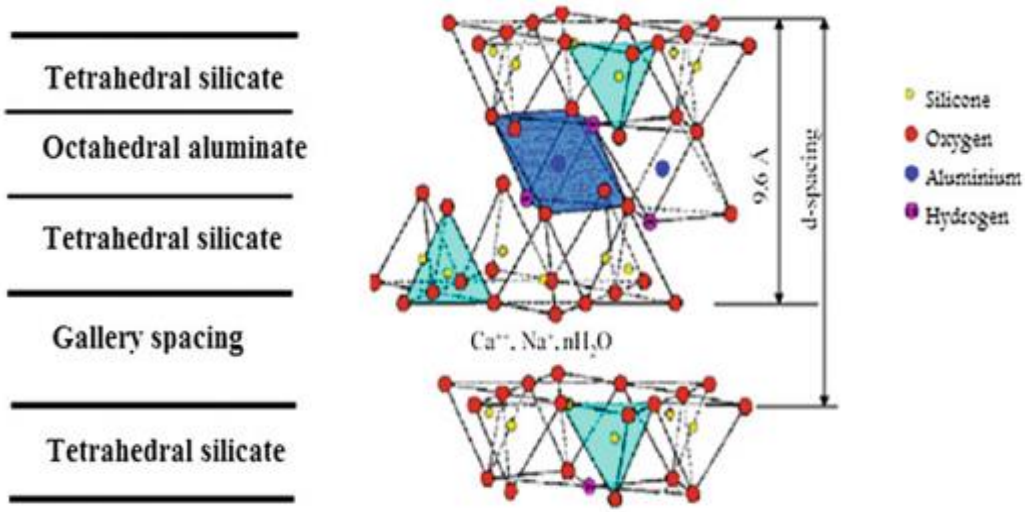

Figure 2.4: Structure of Montmorillonite (Visakh, et al., 2013)

From Figure 2.4, each layer is connected by Van der Waals force. The main source of charge for MMT is from isomorphic substitution. Isomorphic substitution happens when some atoms are replaced by other atoms with different valence electrons during growth of the crystal structure. For examples, the substitution of Al^{3+} for Si^{4+} in the tetrahedra and Fe^{2+}, Mg^{2+}, and others for Al^{3+} in octahedra within clay minerals. Thus, the isomorphic substitution of metal ions will produce extra negative charges. These charges will be balanced by metal cations such as calcium (Ca^{2+}), zinc (Zn^{2+}) and sodium (Na^{+}) in hydrate form in which increases the hydrophilic character (Paul, 2008). This further explains why MMT is compatible with water-soluble polymer. MMT can also disperse into hydrophobic polymer by

organically modified by exchange the inorganic metal ions with quarternary alkyl ions.

MMT has outstanding properties such as high surface area, high aspect ratio and highly reactive. It is easy to be modified by organic to help it disperse in polymer matrix and occurs in large amount in nature. All this contribute to its importance as reinforcement in polymers. MMT usually mixed with polymers at filler loading level, usually 1-5 wt% (Majeed, et al., 2013).

MMT is incorporated into polymer matrix in two manners depending on the degree of penetration, namely intercalated and exfoliated (Schulz, Kelkar and Sundaresan, 2005). Intercalated system is where the layered structure of MMT is filled alternating with polymer layers and spacing larger than that of original MMT. A separation process called intercalation will allow the polymer molecules to enter into the clay platelets. In exfoliated systems, the MMT is first organically modified, then delaminated into nanometer MMT where promote dispersion into polymer matrix. In exfoliated system, the MMT nanofillers have nanometer sized flexible structure. Figure 2.5 below shows the difference between intercalation and exfoliated system. The first possible structure showing the phase separated is incorporated in microcomposites while intercalated and exfoliated systems are exists in nanocomposites.

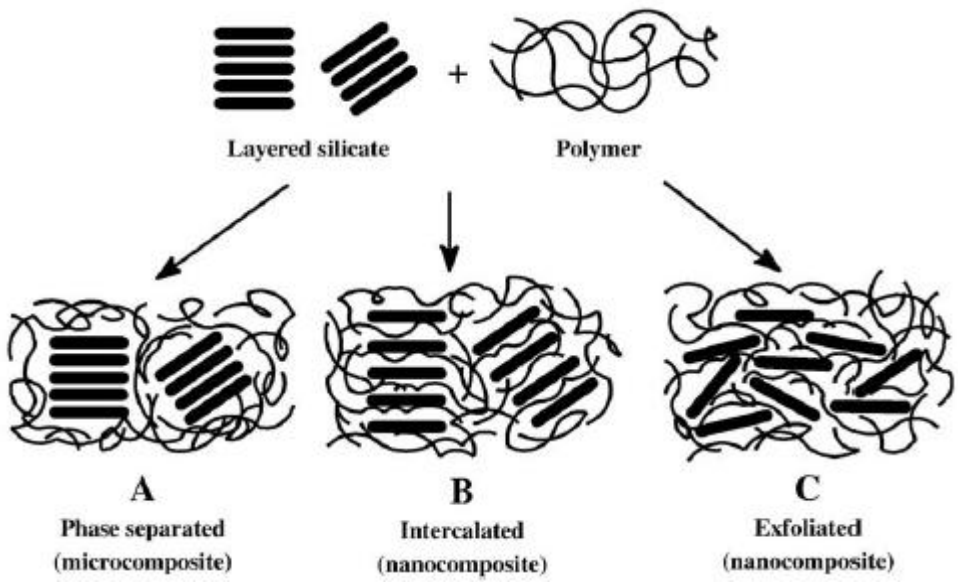

Figure 2.5: Three Types of Composite Structures (Tunc and Duman, 2010)

2.5 PVOH-natural fibers composites

Many researches had been done to find out which natural fibers are compatible with PVOH to give the optimum mechanical and thermal properties while reducing the production cost of PVOH.

2.5.1 PVOH - sugarcane bagasse cellulose composite

Study done by Mandal and Chakrabarty (2013) obtained nanocellulose from sugarcane bagasse through sulphuric hydrolysis isolation process. They established that blending of PVOH with water sugarcane bagasse nanocellulose showed an increase in tensile strength and elongation at break with increasing nanocellulose composition as shown in Figure 2.6 and Figure 2.7 below respectively. Improvement of tensile strength might due to high compatibility between the nanocellulose and the PVOH polymer matrix causing homogeneous distribution of the nanocellulose in the matrix, wide hydrogen bonding and high interfacial surface area. However, the elongation at break increased up nanocellulose of 5 wt% and then decreases beyond that. For nanocellulose more than 5 wt%, the fibers would tend to aggregate causing reinforcements become ineffective.

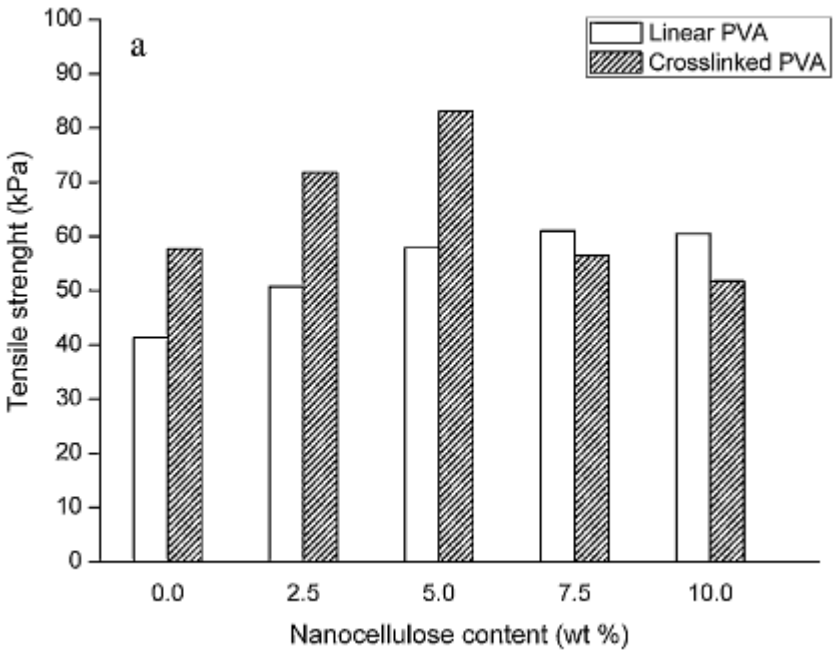

Figure 2.6: Tensile Strength of PVOH (PVA)-Nanocellulose (Mandal and Chakrabarty, 2013)

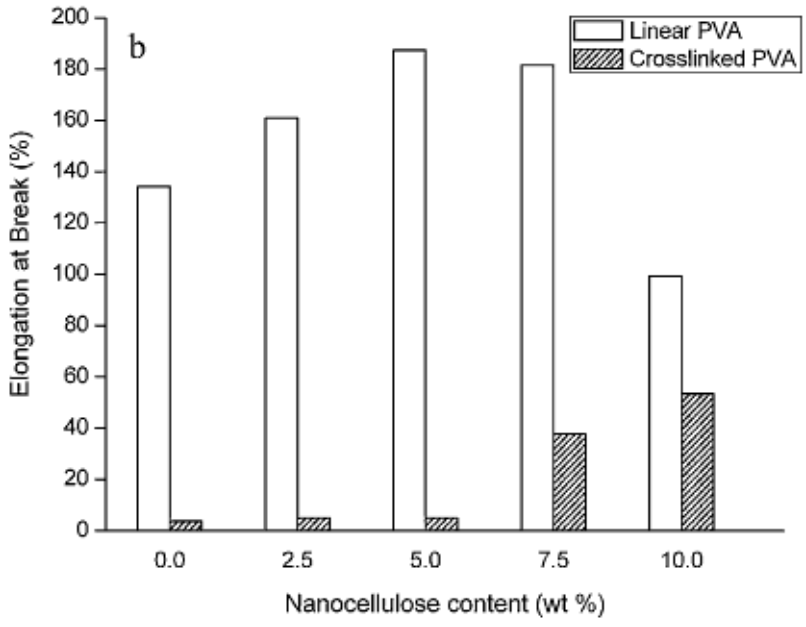

Figure 2.7: % Elongation at Break of PVOH (PVA)-Nanocellulose (Mandal and Chakrabarty, 2013)

Thermogravimetric analysis (TGA) demonstrated weight loss occurs at three main regions as shown in Figure 2.8. The first region of weight loss occured at around 30-140°C in which the physically weak and loosely bound moisture on the surfaces are evaporated. The weight loss is about 10 wt%. Second region occured due to degradation of PVOH-nanocellulose structure at about 220-400°C. Whilst third region happened at above 400°C due to cleavage of the PVOH – nanocellulose nanocomposites and breakdown of carbonaceous materials such as polyene produces a mixture of hydrocarbons and carbon (Jia, et al., 2007). At second stage, the thermogram showed the nanocellulose had increases the thermal stability of virgin PVOH and delayed the degradation rate of the composites due to formation of hydrogen bonds between nenocellulose and PVOH.

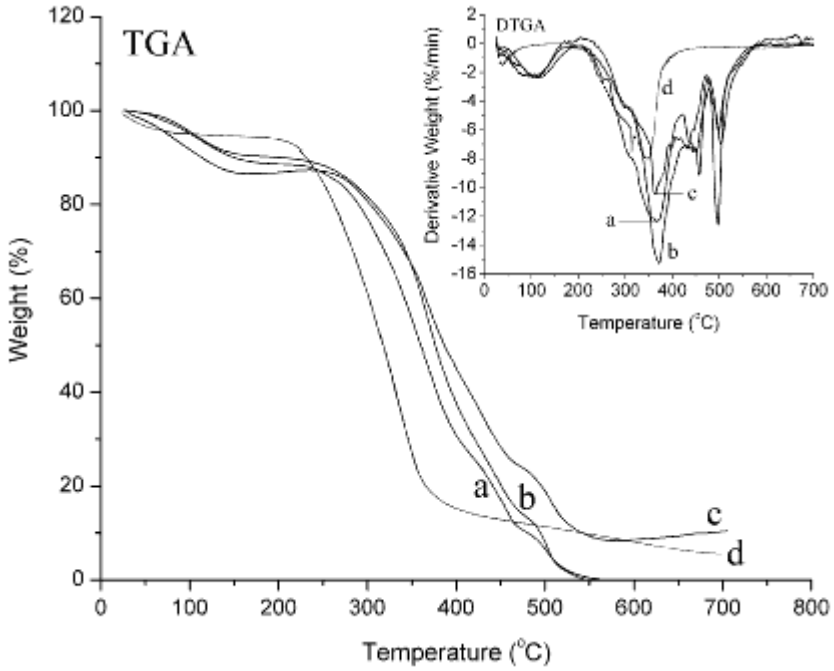

Figure 2.8: TGA Curves for PVOH-Nanocellulose Composites (Mandal and Chakrabarty, 2013)

At the same time, differential scanning calometry (DSC) as shown in Figure 2.9, showed that the melting temperatures of the PVOH-nanocellulose composites is lower compared to virgin PVOH. Another significant difference was that pure PVOH had sharp peak while PVOH-nanocellulose composites crystallized at a range of temperatures. This was due to the behaviour of crystals of the structure. Pure PVOH

has crystallites with uniform order and size. Therefore, pure PVOH melted very sharply over a narrow range. Whereas composites has crystallites with different size leading to melting happens over a wide range of temperature.

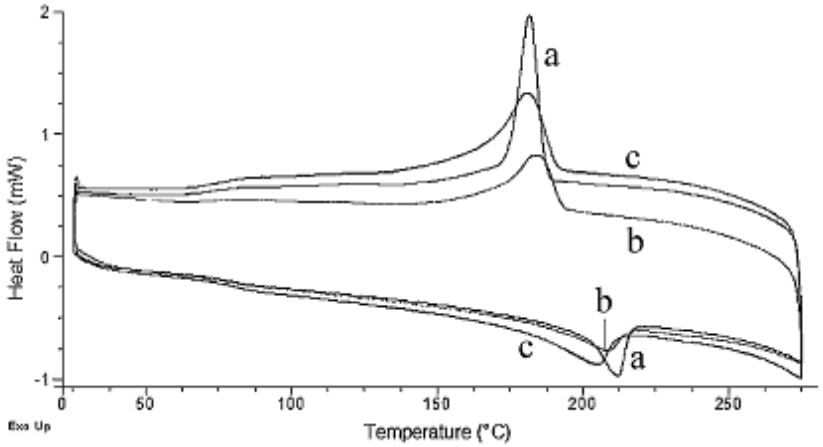

Figure 2.9: DSC Thermogram for PVOH-Nanocellulose Composites (Mandal and Chakrabarty, 2013)

X-ray diffraction (XRD) as shown in Figure 2.10 below showed the both pure PVOH and composites are characterized by a sharp peak at 2θ = 19.3° which represented the characteristics of PVOH. Peaks of nanocellulose which is at 2θ = 22.5° is not found from 5 wt% of nanocellulose proved that nanocellulose was present in insignificant amount in the composite. For nanocellulose of 10 wt%, the peak of cellulose was found weakly at 2θ = 21.6°, in which appeared to be shifted towards left.

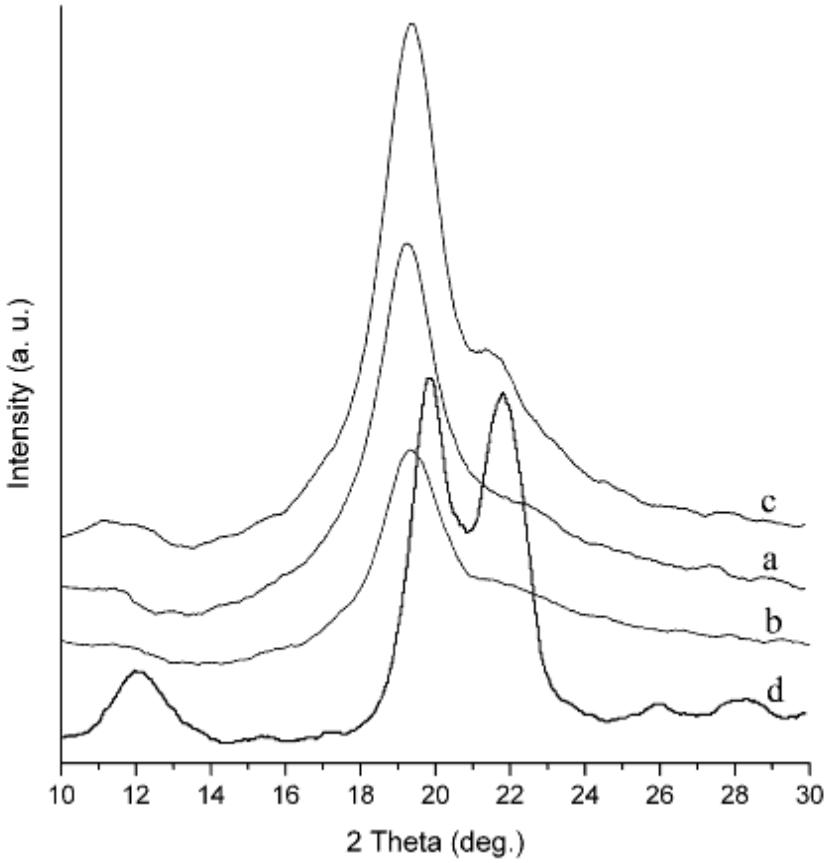

Figure 2.10: XRD of PVOH and PVOH-Nanocellulose Composites (Mandal and Chakrabarty, 2013)

As can be seen from Figure 2.11 below, when the amount of nanocellulose particles in the PVOH matrix was increased to 10 wt%, the nanocellulose would agglomerate and form spherical droplets. Thus, this can further support why mechanical properties especially percentage of elongation at nanocellulose reinforcement of 10 wt% did not improve much compared to nanocellulose of 5 wt%.

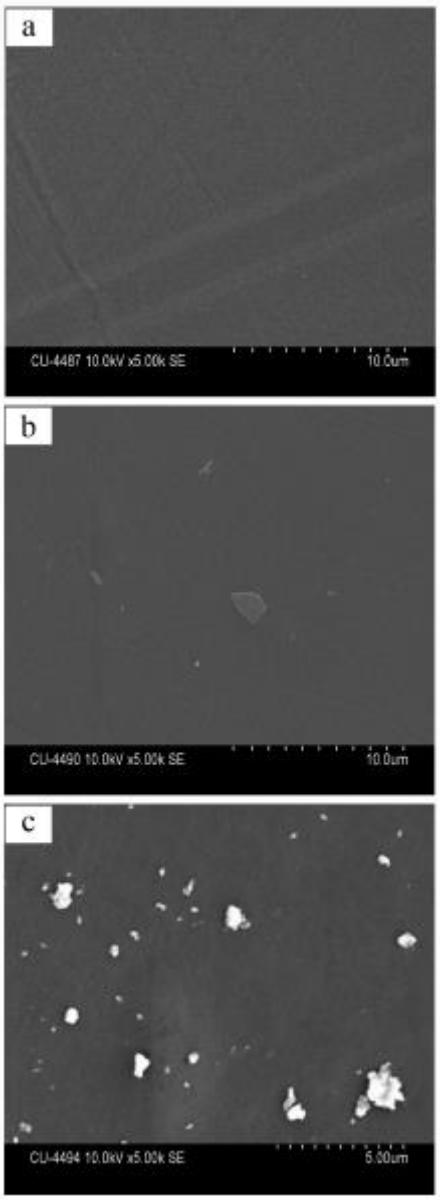

Figure 2.11: SEM Images of PVOH and PVOH-Nanocellulose Composites (Mandal and Chakrabarty, 2013)

Fourier transform infrared (FTIR) spectra of PVOH-nanocellulose composites were shown in Figure 2.12 below. According to studies by Kondo et al. (1994), they identified two main kinds of hydrogen bonding as shown in Figure 2.13 below. First, is the hydrogen bonding between –OH from PVOH and –OH at the C-2 or C-3 position in the glucose ring. Second, is the hydrogen bond formed between the –OH from PVOH and ring oxygen O-5 from in the glucose ring. An absorption band at about 2917 cm^{-1} was seen in the spectra. This is due to the C-H and CH_2

stretching vibrations from alkyl groups of PVOH and nanocellulose. Peak at 3250 cm^{-1} was contributed by the free O-H stretching vibration from the intermolecular and intramolecular hydrogen bonds within PVOH itself and also between hydroxyl (-OH) groups of PVOH and cellulose. On the other hand, a broader band at 3400 cm^{-1} was observed which is attributed by the O-H stretching vibration of the –OH groups in nanocellulose. It was found out that when nanocellulose is introduced into PVOH, it has a slight effect on the intensity of O-H stretching. This is because the nanocellulose loading is too low to give a marked effect although the -OH groups on the surface in the PVOH matrix through secondary valence bond formation. The interaction between PVOH and nanocellulose can be proven by the peak at 850 cm^{-1} which appear in the PVOH spectra but was not seen any in cellulose spectra. The absorption band of PVOH at 850 cm^{-1} was slowly lessened with increasing loading of nanocellulose. In addition, the absorption band at around 1060 $cm^{-1}$is a distinctive peak for nanocellulose attributed by the C-O-C ring due to the interaction between –OH of PVOH and the ring oxygen O-5. In PVOH-nanocellulose composites, the intensity of this peak increased with increasing nanocellulose content supported the interaction between PVOH and nanocellulose.

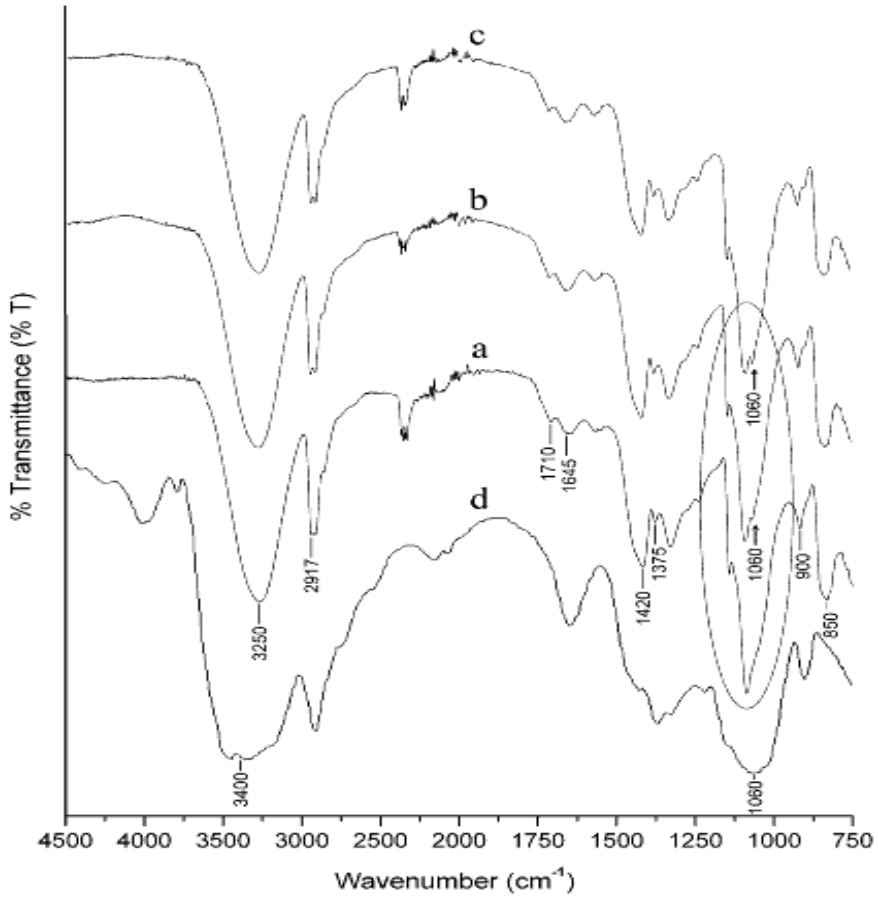

Figure 2.12: FTIR Spectra of PVOH-Cellulose Composites; Pure PVOH (a), 5wt% Nanocellulose (b), 10wt% Naocellulose (c) and Nanocellulose (d) (Mandal and Chakrabarty, 2013)

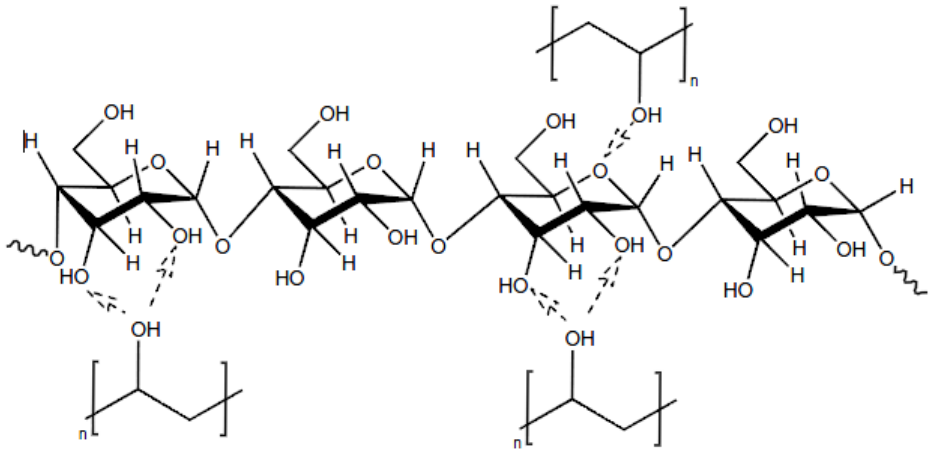

Figure 2.13: Possible Hydrogen Bonding between PVOH and Cellulose (Kondo et al., 1994)

2.5.2 PVOH - hydroxypropyl cellulose blend

Hydroxylpropyl cellulose (HPC) is a type of cellulose ether which is soluble in water and polar organic solvents. Guirguis and Moselhey (2011) reported that increase of HPC in PVOH would decrease the glass transition temperature. The broadening of OH peaks declined. This showed that the hydroxyl groups of PVOH are highly interconnected by hydrogen bonding, contributing to high glass transition temperatures. However, the heat of fusion and melting temperature decreased with increasing HPC added. This is because when HPC is added into PVOH, the crystal structure was disordered, thus reduction of the crystallinity of the structure caused decreases of the enthalpy of phase change. Table 2.2 below shows the glass transition temperature, melting temperature and crystallinity index.

Table 2.2: Transition Temperatures, Melting Temperatures and Crystallinity Index (Guirguis and Moselhey, 2011).

PVOH-HPC (wt/wt%)	Transition temperature, T_g (°C)	Melting temperature, T_m (°C)	Crystallinity index
100/0	88.1	209.6	47.170
90/10	87.8	206.1	52.525
75/25	93.9	221.7	49.979
50/50	95.4	197.5	36.905
25/75	75.1	203.1	31.646
0/100	83.9	-	-

2.5.3 PVOH - microfibrillated cellulose composite

Qiu and Netravali (2012) suggested that the microfibrillated cellulose were well bonded to PVOH and uniformly distributed throughout the PVOH matrix. This contributed to higher thermal stability of PVOH- microfibrillated cellulose composites. Another study by Tanpichai, Sampson and Eichhorn (2014) used lyocell

fibers to produce microfibrillated cellulose. They proved that the presence of microfibrillated cellulose in PVOH enhanced the Young's modulus and tensile strength of the composites up to 3 wt% of fibrils as well as thermal degradation. Lu, Wang and Drzal (2008) also reported that microfibrillated cellulose from kraft pulp by mechanical process incorporated into PVOH showed an improvement in Young's modulus and tensile strength until reach an optimum at 10 wt% of microfibrillated cellulose. The thermal stability increased as well.

2.6 Polymer-kenaf nanowhisker nanocomposites

Many researchers had incorporated kenaf nanowhisker into polymer and tested their compatibility and changes in properties such as mechanical and thermal.

2.6.1 Polylactic acid (PLA)-kenaf and polypropylene (PP)-kenaf nanocomposites

Ochi (2008) found out that the tensile strength and flexural strength of kenaf-polylactic acid (PLA) nanocomposites, increased linearly with fiber up to 50%. He also proved that kenaf fiber showed higher tensile and flexural strength as compared to other natural fibers when incorporated into PLA. Ochi's statement was further proven by Seong, et al. (2012). As we can see from Figure 2.14 below, the flexural strength of composites of kenaf-polypropylene (PP) and kenaf-polylactic acid (PLA) were higher than virgin PP and PLA. The modulus was also increasing in both polymers with increasing amount of fibers added because kenaf have higher modulus due to high cellulose content.

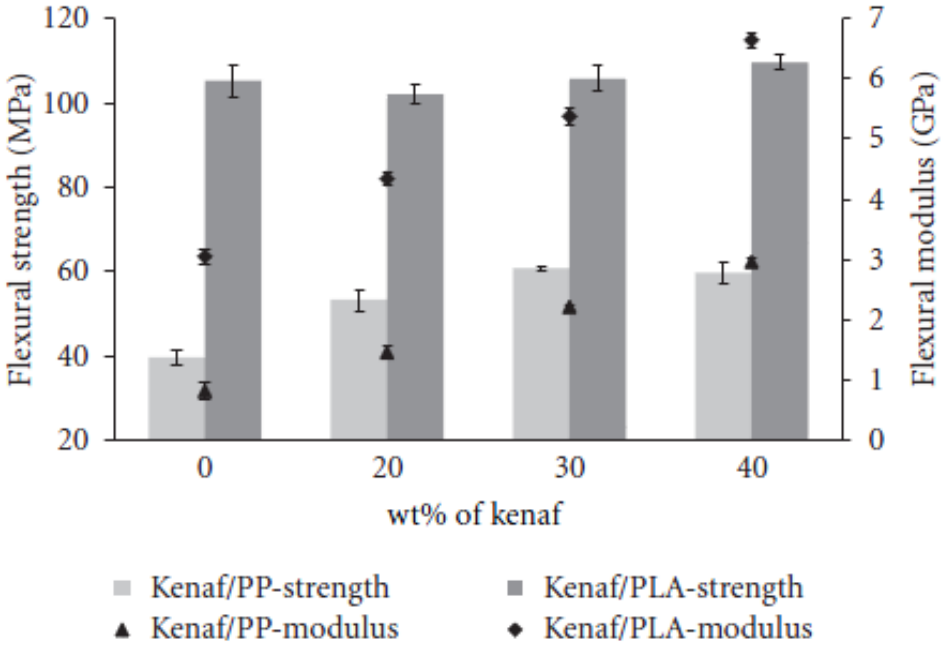

Figure 2.14: Flexural Strength and Modulus of Kenaf-PP and Kenaf-PLA Composites (Seong, et al., 2012)

2.6.2 Polyvinyl chloride (PVC) -Thermoplastic polyurethane (TPU) – kenaf nanocomposite

In contrast, El-Shekeil, et al. (2014) in their research found out that when kenaf was incorporated into polyvinyl chloride (PVC)-thermoplastic polyurethane (TPU) composites, the tensile strength was decreased with increasing fiber content. Fibers function as stress transfer in the polymer matrix. Enhancement of tensile strength in composites depends greatly on effective and uniform stress distribution (Özturk, 2010). Theoretically adding fibers with higher strength to the matrix with lower tensile strength should give composites with increasing tensile strength if interfacial bonding is good. At this case, the tensile strength of composites added with kenaf decreased. This decrease in the tensile strength was due to the poor fiber-matrix interfacial bonding. The fiber-matrix poor linkage was further supported by morphology observations. The elongation at break decreased as well when amount of kenaf added increased from 20 wt% to 40 wt%. At low kenaf loading, the high strain rate was due to the composite is assumed to behave like PVC-TPU nature where

kenaf only contribute to little or even no effect to strain rate. This is stated by Kim, et al., that most polymeric materials have a tendency to be strain-rate dependent. At high fibers content, poor fibers-matrix bondings will cause failure to occur faster. On the other hand, the increase of modulus with increasing of fiber content was attributed to higher stiffness of the kenaf fibers than the matrix. The decrease in strain with increasing fiber amount was caused by the low elongation of fibers. Figure 2.15 below shows the effect of kenaf on tensile properties of PVC-TPU-kenaf composites.

The standard deviation for strain curve is very large in the 20 wt% kenaf loading as can see from Figure 2.15. By increasing the fiber amount, the standard deviation is getting less. In low fiber content, lesser fibers particles are available in the matrix, thus, there will be lesser fibers at some points than other points. Points with low fibers content will have higher elongation while points with high fibers content result in less elongation as reason stated above. This explains why the standard deviation is high in 20 wt% kenaf loading. When the fiber content is increased, more fibers are available to be distributed in the matrix. Therefore, the matrix would not have the problems where some points with lesser fibers while other points have more fibers. This is why higher kenaf fibers content results in lower standard deviation in strain curve.

In terms of thermal stability, thermogravimetric analysis (TGA) showed that thermal degradation took place in three steps. In first step, matrix had similar stability as composites where evaporation of absorbed moisture occurred from 25°C to 188°C. At second step, lower fiber content had a higher thermal stability than higher fiber contents in which decomposition of hemicellulose occurred from 188°C to 500°C. At last step, composites exhibited better stability than the matrix. This showed the kenaf fibers improved the composites' thermal stability at higher temperatures.

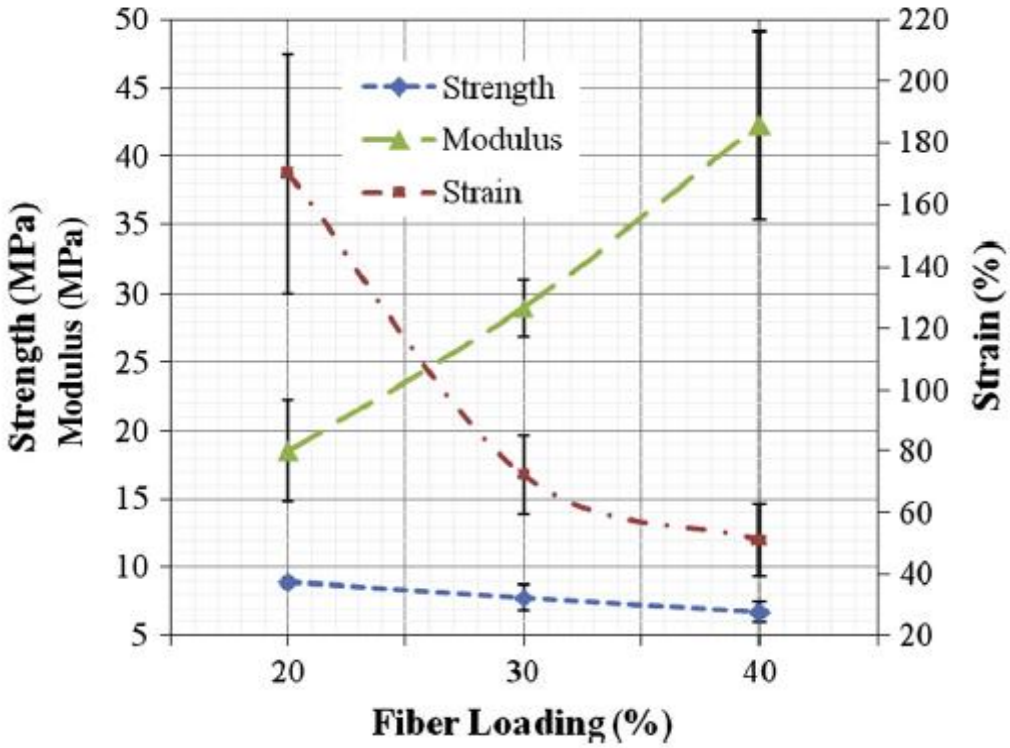

Figure 2.15: Effect of Fiber Content on Tensile Properties of PVC-TPU-Kenaf (El-Shekeil, et al., 2014)

2.6.3 PVOH – kenaf nanocomposite

Besides, kenaf nanowhisker also had been incorporated into polyvinyl alcohol (PVOH) in study by Shi et al. (2011). They found out that the incorporation of kenaf nanowhisker into PVOH was optimum at 9 wt% as shown in Figure 2.16 below. From scanning electron magnification (SEM) images, cracks were formed before failure at any composition. However, most cracks grew in composites with 9 wt% kenaf nanowhisker. These cracks were consistent with high energy absorption. The hydrogen bonding formed between kenaf nanowhisker and PVOH contributes to high inter-laminar shear strength which allows cracks to form. Shi et al (2011) also found out that the kenaf bast fiber used in their study had greater tensile strength enhancement than those from flax bast fiber used in Bhatnagar and Sain's (2005) study. However, the reinforcement from kenaf fiber was lesser compared to those from rutabaga and hemp (Lee, et al., 2009).

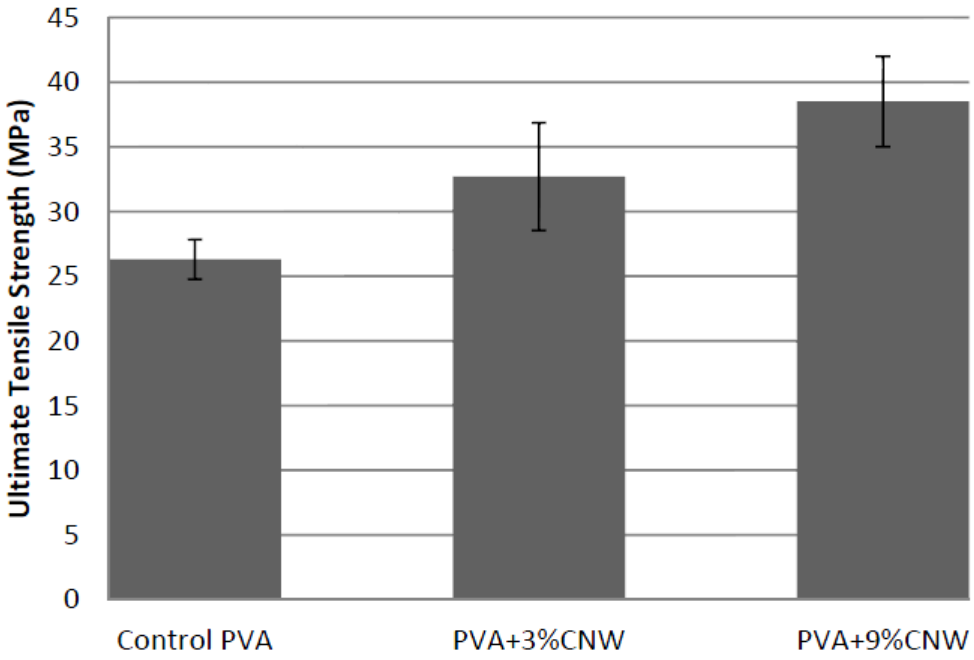

Figure 2.16: Tensile Strength of Kenaf Nanowhisker-PVOH (PVA) Composites (Shi, et al., 2011)

2.6.4 Other nanocomposites

Helbert, Cavaille and Dufresne (1996) found out that 30 wt% of wheat straw cellulose whiskers incorporated into poly(S-co-BuA) latex film exhibited an outstanding Young‘s modulus of more than 1000 times higher compared to virgin polymer. This improvement was not only due to structure and toughness of the nanocellulose, but also attributed to the formation of hydrogen bonding.

Overall, each type of natural fibers processed in different ways produce reinforcing nanocomposites with different mechanical properties. Mechanical properties of natural fibers can be affected by many factors, such as fiber chemical composition, cell dimension, compatibility of fibers with polymer matrix and others. Table 2.3 below shows the mechanical properties of some commonly used natural fibers. Among all, kenaf fiber is considered as one of having the highest tensile strength, Young’s modulus and moderate elongation at break.

Table 2.3: Mechanical Properties of Natural Fibers (Omar, et al., 2012)

Fiber	Tensile strength (MPa)	Young's modulus (GPa)	Elongation at break (%)
Abaca	400	12	3-10
Bagasse	290	17	-
Bamboo	140-230	11-17	-
Flax	345-1035	27.6	2.7-3.2
Hemp	690	70	1.6
Jute	393-773	26.5	1.5-1.8
Kenaf	930	53	1.6
Sisal	511-635	9.4-22	2.0-2.5
Ramie	560	24.5	2.5
Oil palm	248	3.2	25
Pineapple	400-627	1.44	14.5
Coir	175	4-6	30
Curaua	500-1150	11.8	3.7-4.3

2.7 Polymer – MMT nanocomposites

MMT is usually incorporated in water-soluble polymers such as PVOH and polyethylene oxide. For example, PVOH - MMT nanocomposites were prepared by using solution-intercalation casting method. The MMT exists as colloidal suspension in PVOH water solution. When the solution is dried, silicate layers of MMT is distributed and surrounded by the polymer matrix. Further drying causing water in the suspension to evaporate, the polymer will traps the MMT layers apart and thus MMT can remains dispersed in the polymer matrix.

2.7.1 PVOH-MMT composite

Strawhecker and Manias (2000) commented that all composites before failure would undergo a period of elastic deformation followed by an increasing stress during plastic deformation. The results of tensile test showed Young's modulus increased sharply with increasing MMT loading at very small MMT amount and when more than 4 wt% of MMT was added, subsequently the Young's modulus dropped. This behaviour has been stated earlier for poly-(dimethylsiloxane)-MMT exfoliated composites. The improvement of the Young's modulus for very low MMT loading was not simply due to the incorporation of the higher modulus inorganic filler layers. A theoretical approach is assuming a layer of affected polymer on the filler surface, with a much higher Young's modulus than the bulk polymer. This affected polymer can be assumed of as the points of the polymer matrix that is physically absorbed on the silicate surfaces, the bond and attraction to the filler clay surfaces make the polymer become stiffer. Clearly, the aspect ratio of MMT is high contributing to the large surface area exposed to polymer and thus the sharp increases in the modulus with very low MMT loading were expected. For MMT loading above 4 wt%, the MMT existed as exfoliated layers in the polymer matrix that the structure were already changed by other MMT layers, thus the increment of Young's modulus was much less significant. The elongation at break decreased as expected due to the brittleness of the nanocomposites after incorporated with MMT. Figure 2.17 below shows the Young's modulus, tensile strength, toughness and strain at break of the PVOH-MMT composites.

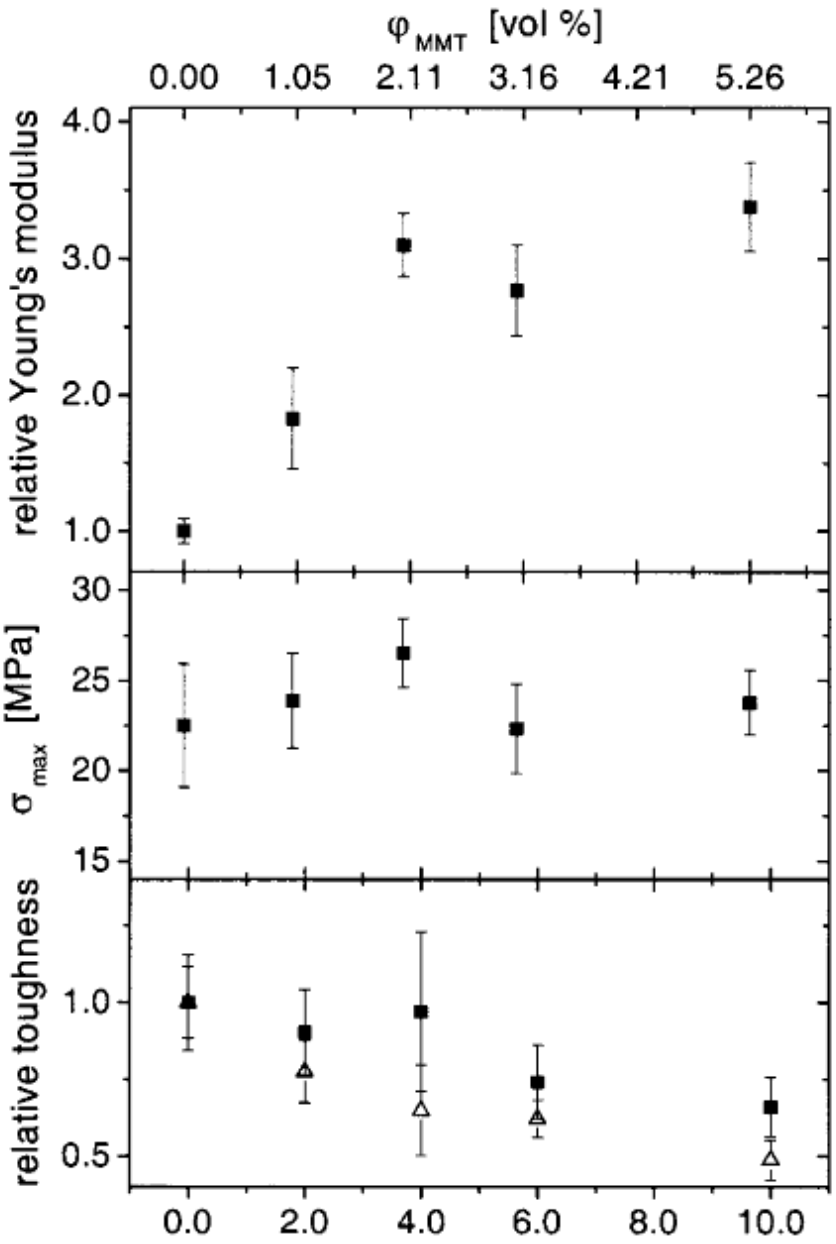

Figure 2.17: Young's Modulus, Maximum Stress at Break, Toughness (Squares) and Strain at Break (Triangles) of PVOH-MMT Composites (Strawhecker and Manias's, 2000)

Besides, transmission electron microscopy (TEM) images showed that there was coexistence of intercalated and exfoliated stated of silicate in PVOH for 20 wt% MMT. Yet, at low MMT concentration, the MMT layers were well dispersed within the PVOH matrix, which means the nanocomposites were mostly in exfoliated form. Both their distributions and d-spacings decreased with increasing MMT content, from 40 wt% to 90 wt % MMT. Figure 2.18 below shows the TEM image of 20%

MMT-PVOH nanocomposites revealing the coexistence of intercalated (A) and exfoliated (B) MMT layers.

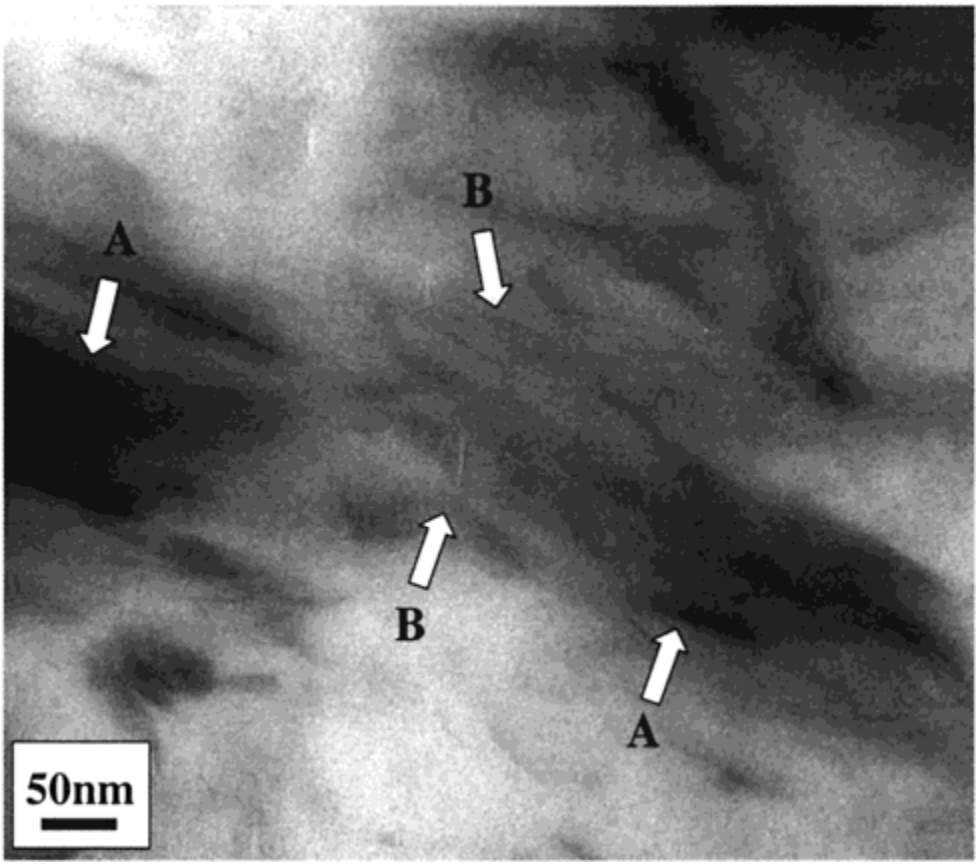

Figure 2.18: TEM Images of 20% MMT-PVOH Nanocomposite (Strawhecker and Manias's, 2000)

From study by Strawhecker and Manias (2000), an important property was found that for nanocomposites contains more than 60 wt% MMT, there was no thermal transitions can be detected between transition temperature, Tg and melting temperature, Tg of pure PVOH. Both Tg and Tm were too broad to be measure in fully intercalated nanocomposites. However, at low MMT loading (<60 wt%), both the melting temperature and enthalpy of melting increased with higher MMT loading. This means PVOH-MMT nanocomposite has higher thermal stability. The weight loss as a result of the degradation of PVOH until the temperature of about 275 °C was approximately the same for both pure PVOH and also PVOH-MMT composites as shown in Figure 2.19 below. After this temperature, the composites exhibits

higher thermal stability as the MMT layers prevents the PVOH weight loss, which influences a maximum delay of approximately 75 °C.

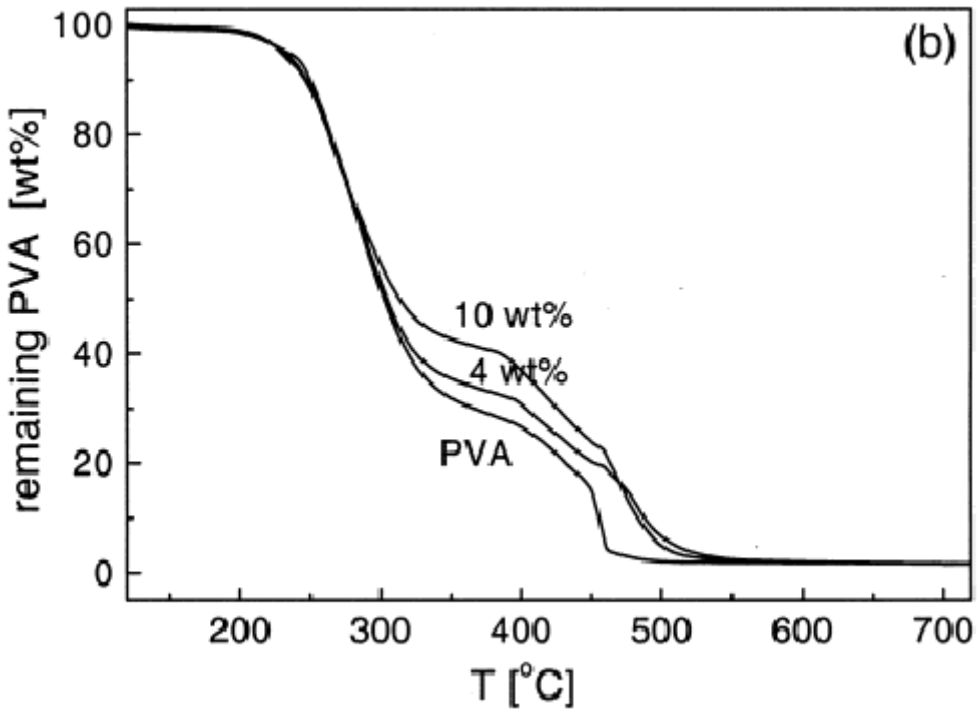

Figure 2.19: TGA Curves for PVOH-MMT Composites (Strawhecker and Manias's, 2000)

In further support Strawhecker and Manias's (2000) research, Liu, et al. (2014) found out that the tensile strength of PVOH–Na^+-MMT enhanced considerably compared to pure PVOH. He explained this was due to ultra-high interfacial interaction and ionic bonds between PVOH matrix and Na+-MMT generated from uniform dispersion of the nanosize clay particles. Other types of MMT including di-hydrogenated tallow ammonium/siloxane (I.44PSS) organically modified MMT, 18-amino stearic acid (I.24TL), methyl, bis hydroxyethyl, octadecyl ammonium (I.34TCN), dimethyl, also has been incorporated into PVOH polymer matrix. Nevertheless, the PVOH–I.34TCN and PVOH–I.34TCN showed decrease in tensile strength. This showed that the I.34TCN and I.34TCN were hydrophobic in nature, thus were not compatible with and cannot disperse well in the hydrophilic PVOH matrix. After incorporation of Na^+-MMT, the PVOH polymer became brittle

which play a role as bridge interacting PVOH chains. Hence, the results showed that the elongation at break decreased for PVOH–Na^{+}-MMT composites.

Liu, et al. (2014) reported that the 5 wt% of MMT silicate layers were existed in exfoliated form in PVOH matrix, whereby the MMT layers were further apart (>5nm) and the parallel stacking were lost (Strawhecker and Manias, 2000). Therefore from XRD, no diffraction peak of clay, which is $2\theta = 6.99°$ for Na+-MMT was observed. The XRD analysis results showed that Na^{+}-MMT demonstrates the best interaction with the PVOH polymer.

2.7.2 Polyethylene- acrylic acid (PEAA) zinc salt– MMT composite

The tensile strength enhancement of MMT in polymer was further proved by Li and Sur (2014). They incorporated MMT into polyethylene-co-acrylic acid (PEAA) zinc salt. The tensile strength increased linearly with increasing MMT loading from 0 wt% to 10 wt%. The Young's modulus of the PEAA added with MMT nanocomposites increased as well with increasing filler content. This was due to both the structure of PEAA and the linkage of PEAA polymer chains formed by the Zn^{2+} ions needed to be broken down. Next, at 1 wt% MMT loading, the elongation at break was enhanced compared to pure PEAA but decreased with further increasing of Zn^{2+}–MMT loading. This attributed to the aggregation of MMT and increase in stress concentration when amount of MMT was increasing in the PEAA polymer, caused nanocomposite become more brittle and thus the nanocomposite is easier to fail. Conclusion for this study is that loading of MMT at 1 wt% in PEEA is the best as it improves all the mechanical properties including tensile strength, elongation at break and Young's modulus.

From Li and Sur (2014) study, the Zn^{2+}–MMT particles were well dispersed within the PEAA matrix and the silicate layers of MMT were prolonged by PEAA forming intercalative and exfoliated structure. The d-spacing of PEEA matrix decreased with increasing MMT amount in the PEAA matrix. This showed the PEAA were intercalated into the silicate layers. This was predictable because

intercalation of preferable for higher clay content. In contrast, the intensity of MMT peak was quite weak in the nanocomposite, indicating that exfoliated form was the dominant form of the clay in the PEAA matrix.

Report by Li and Sur (2014) also indicates that the polyethylene-co-acrylic acid (PEAA) zinc salt incorporated with MMT has slow down the degradation of particles of PEAA at high temperatures. This is because the zinc cations from MMT will interact with carboxyl groups from PEAA to form strong electrostatic interactions. As shown in Figure 2.20 below, degradation of PEEA incorporated with MMT happened at two stages. First, the ammonium from treated PEEA with ammonium hydroxide are released at 140°C. At second stage, polymer chains are being cut into shorter chains in which the scission is through processed called pyrolysis and depolymerisation occurred at 469°C.

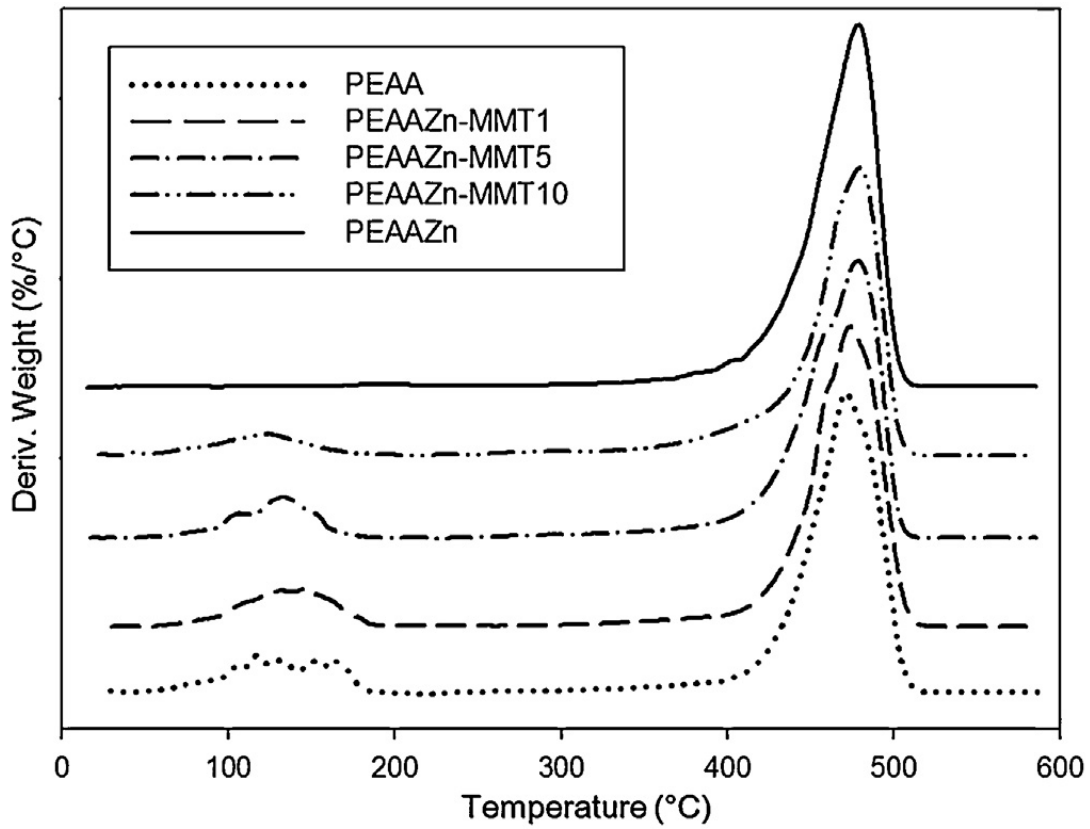

Figure 2.20: TGA Curve of PEEA-MMT Nanocomposites (Li and Sur, 2014)

2.8 Cellulose based-MMT nanocomposites

Recently, cellulose-based nanocomposite films were in interest due to its biodegradable and environmental friendly properties. Moreover, these natural fibers are cheaper than biodegradable synthetic polymers. These cellulose-based materials are biocompatible, thus increasing its demand by many industries (Johansson, et al., 2012). In recent times review journal on consumption and development of bio-fibers for packaging applications have defined some of the main problems. These natural fiber filled polymer composites still not able to replace synthetic polymers in every packaging applications due to low mechanical properties, hydrophilic character, degradability especially under humid atmospheres. Thus, many research has been done or under development to find a solution to overcome these inferiors. One of the researches is from Yang, et al. (2012). They have done a research on hydrophilic cellulose-based nanocomposites produced from lithium hydroxide (LiOH)-urea-cellulose (LUC) solutions incorporated with montmorillonite (MMT) clays as reinforcement to enhance their thermal stability and mechanical properties.

The stress-strain graph showed that both tensile strength and Young's modulus of the nanocompoaites increased to about twice than that of the pure LUC when 15 wt% of MMT is added. This indicates that the MMT can layers were distributed well in the LUC matrix. However, the elongation at break decreased when loading of MMT increased due to MMT is more brittle than tough and ductile cellulose. Thus, incorporation of MMT into cellulose decreased the ability of cellulose to absorb energy prior to failure (Chen and Zhang, 2006). Improvements of mechanical properties of nanocomposites were further supported by the development of ordered intercalated layered structures of MMT in the cellulose matrix. The d-spacing of MMT increased to 1.6 nm in the LUC-MMT nanocomposites when the cellulose loading was increased to 95%, indicating the formation of intercalated structures of MMT layers in the cellulose matrix. The 1.6 nm d-spacing of MMT in the LUC-MMT naocomposites were 0.4 nm larger than that of the pure MMT clays which is 1.2 nm, which agreed to the presence of a single layer of cellulose particles between the MMT layers (Ebina and Mizukami, 2007).

Majdzadeh and Nazari (2010) had done a research producing nanocomposites from adding PVOH and MMT into thermoplastic starch. They found out that addition of MMT will disrupt the bonding between starch matrix and PVOH through fourier transform infrared (FTIR) analysis. Pure thermoplastic starch has a peak due to the O-H stretching at 3315 cm^{-1}, while the thermoplastic starch – PVOH – MMT has a higher wavelength peak at 3320 cm^{-1}, indicated that PVOH has higher preference to interact with MMT.

Research by Dean, et al. (2007) further support the fact that addition of nanoclay will disrupt the bonding between cellulose matrix and PVOH. When nanoclays are added into startch - PVOH composites, the –OH band shifted from 3295 to 3305 cm^{-1}shows that there is strong interaction between the PVOH and MMT in the nanocomposites.

CHAPTER 3

METHODOLOGY

3.1 Materials

3.1.1 Polyvinyl alcohol (PVOH)

Fully hydrolysed polyvinyl alcohol (PVOH) produced by Sekisui Chemical Co. Ltd was used in this study.

3.1.2 Montmorillonite (MMT)

Nano-size montmorillonite (MMT) clay brand name is Nanolin DK purchased from HangZhou Sino-Holding Chemicals Co., Ltd.

3.1.3 Kenaf nanowhisker

The kenaf used to produce kenaf nanowhisker was purchased from J&Z Agrofarm at Saleng, Johor. Other chemicals that are needed in preparing the kenaf nanowhisker include sodium hydroxide (NaOH), sulphuric acid (H_2SO_4) and sodium chlorite, ($NaClO_2$). Sodium hydroxide and sodium chloride were bought from Fisher

Scientific (M) Sdn. Bhd. while sulphuric acid was bought from See Sen Chemical Bhd. The preparation steps of kenaf nanoshiwker are as below.

Kenaf nanowhisker was prepared using alkali treatment followed by acid hydrolysis. Initially, kenaf fibers was stirred in a 4 wt/wt% sodium hydroxide, NaOH solution at 80°C for about 3 hours to remove most of the lignin and hemicellulose. This step was repeated for three times. Then, bleaching treatment was performed three times with 1.7% sodium chlorite, $NaClO_2$ solution and acetic acid buffer solution for 4 hours at 80°C to remove the remaining lignin. To remove amorphous regions, acid is used because amorphous is susceptible to acid attack. Acid hydrolysis was conducted at 45°C with 65% sulphuric acid, H_2SO_4. The hydrolysis time was fixed at 40 minutes, which is established earlier to be ideal by Kargarzadeh, et al. (2012). The process was terminated by placing the reaction flask into an ice bath. The excess sulphuric acid was then removed by repeated centrifugation at 10,000 rpm for 10 minutes. The resulting suspension was dialysed against distilled water using a cellulose membrane for about 1 week. The final suspension was of pH6.

Figure 3.1 below shows the main steps in preparation of kenaf cellulose nanowhisker:

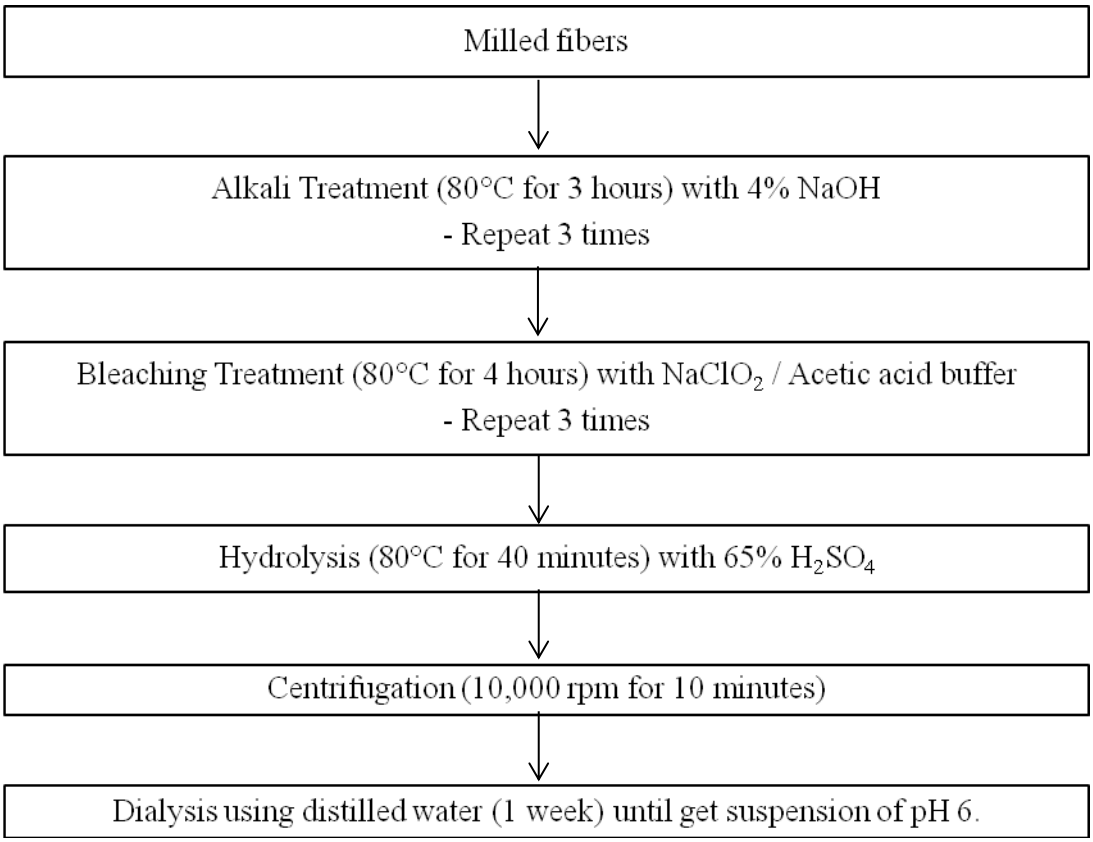

Figure 3.1: Main Steps Involved in Preparation of Kenaf Nanowhisker

3.2 Formulation

The amount of PVOH used was fixed at 10*g* and as basis for other additives. The kenaf nanowhisker was varied for 4 different compositions, which are 0 phr, 2 phr, 4 phr, 6 phr and 8 phr. While MMT was varied for 3 different compositions, that are 1 phr, 3 phr and 5 phr. Amount of kenaf nanowhisker and MMT are varying for each sample as shown in Table 3.1:

Table 3.1: Formulation of Polyvinyl Alcohol Added with Kenaf Nanowhisker and Montmorillonite

Sample	PVOH (phr)	Kenaf nanowhisker (phr)	MMT (phr)
PKM-0-1	100	0	1
PKM-2-1	100	2	1
PKM-4-1	100	4	1
PKM-6-1	100	6	1
PKM-8-1	100	8	1
PKM-0-3	100	0	3
PKM-2-3	100	2	3
PKM-4-3	100	4	3
PKM-6-3	100	6	3
PKM-8-3	100	8	3
PKM-0-5	100	0	5
PKM-2-5	100	2	5
PKM-4-5	100	4	5
PKM-6-5	100	6	5
PKM-8-5	100	8	5

3.3 Sample Preparation

The solution cast samples of PVOH-kenaf nanowhisker- MMT were prepared. Firstly, PVOH and MMT were mixed and dissolved in 300 mL of distilled water at 97 ± 2°C for 30 minutes using a water bath until all the PVOH dissolved. A motor driven stirrer with speed at about 800 rpm was used to stir the mixtures. The amount of MMT was varied from 1 phr to 5 phr. As the PVOH completely dissolve in distilled water, additional 100 mL of distilled water was added together with kenaf nanowhisker. The amount of kenaf nanowhisker added increases from 2 phr to 8 phr. Then, the mixture of PVOH- kenaf nanowhisker- MMT was heated again in the water bath at the same temperature, 97 ± 2°C for 1 hour. The mixture was cast in the form of film in petri dishes and dried in a vacuum oven at about 65°C for about 48 hours. Few samples were prepared for each test. After that, the samples were sealed in plastic bags and stored under room temperature 25°C at 65% relative humidity for conditioning purpose.

3.4 Sample Testing

3.4.1 Mechanical Properties (Tensile test)

Tensile strength, elongation at break and Young modulus were obtained through tensile test. This test was carried out according to ASTM D 882 standard. The mixtures were cast in the form of standard rectangular-shaped. The specimens' width and thickness were measured. The specimen was placed in the grips aligned in the long axis of specimen. In this test, an Instron mechanical tester (Model: 4206) with tensile tester at crosshead speed of 50 mm/min and a load of 1 kN was used.

3.4.2 Thermal Properties (DSC)

Differential Scanning Calorimetry (DSC) analysis was performed using Mettler Toledo DSC823. The scanning was carried out from 30 °C to 200 °C at a scanning rate of 10 °C/min under dry nitrogen of nearly 100 % purity at a purge rate of 20 mL/min. The DSC thermograms were used to obtain the onset and endpoint melting temperatures for the samples.

3.4.3 Microstructure (SEM and XRD)

Hitachi Scanning Electronic Microscopy of BS 340 TESLA was used to perform the Scanning Electron Microscopy (SEM) analysis to investigate the microstructure of the films, after PVOH is incorporated with kenaf nanowhisker and MMT. The samples were placed on cooper stub and the fractured surface was facing upwards. All the samples were scanned under magnification of ×500, ×1000, ×3000 and ×5000.

The crystallinity structure was observed through X-ray Diffraction (XRD) test using Shimadzu XRD 6000 diffractometer with Cu-Kα radiation (λ= 1.542 Å) for a range of scattering angles 2θ ($3° < \theta < 40°$) at a scan rate of 2° /min. By using 40 kV and 30 mA, the test was implemented with a thin-film attachment that rotated at a speed of 50 rpm.

CHAPTER 4

RESULTS AND DISCUSSION

4.1 Mechanical Properties

Mechanical properties of the nanocomposite samples were evaluated through tensile test. Tensile strength, elongation at break and modulus were determined and calculated from the stress-strain curve. The stress-strain curve for all samples showed that the nanocomposites undergo reversible elastic deformation at beginning, whereby the shape can be returned to original after the force is removed, followed by increasing stress during plastic deformation before failure. The stress-strain curve is non-linear, at the beginning there is a small region with high modulus, beyond which the gradient of curve drops drastically and then the modulus increases again at high strain levels.

4.1.1 Tensile strength

Figure 4.1 shows the tensile strength of PVOH-kenaf nanowhisker-MMT nanocomposites with constant MMT loading. In overall, the tensile result showed a downward trend. When various amount of kenaf nanowhisker were added into PVOH incorporated with 1 phr of MMT, the highest tensile strength was achieved when 2 phr of kenaf nanowhisker was added. The tensile strength increased from 46 MPa to 50 MPa, then level off to 24 MPa when more than 2 phr of kenaf nanowhisker was added. As proven by many researches, cellulose, especially in

nano-sized exhibits stronger and stiffer mechanical properties, thus improved the mechanical properties of their nanocomposites (Majeed, et al., 2013). When 2 phr of kenaf nanowhisker was added, the increment of tensile strength indicates that there is reinforcement of the relatively compliant PVOH matrix with the stronger kenaf nanowhisker. The hydrogen bonds between PVOH and kenaf nanowhisker show good compatibility as both contains hydroxyl group interfacial. In this case, kenaf nanowhisker formed a percolating network with the PVOH matrix and acts as load bearing component. These intermolecular forces keep the stress applied be transferred to kenaf nanocellulose resulted in increment of the mechanical strength of the nanocomposites. For loading of kenaf nanowhisker higher than 4 phr, the tensile strength began to drop. The adverse effect of this kenaf nanowhisker was due to the uneven distribution of the kenaf nanoparticles in PVOH matrix. At high concentration, the nanowhisker particles started to agglomerate. The kenaf nanowhisker tends to form hydrogen bonding within themselves rather than with PVOH causing agglomeration. As agglomeration occurs, the effective aspect ratio decreases, the particles disturb the regular chain of PVOH, forming irregular arrangement. The intermolecular forces became weaker as the aspect ratio was decreasing, lesser energy was required to break the intermolecular forces causing reduction of tensile strength.

When the amount of MMT was fixed at 3 phr, the increasing kenaf nanowhisker loading decreases the tensile strength. This is because tensile strength is highly dependent on the uniform and effective stress distribution (Ozturk, 2010). At 3 phr of MMT loading, kenaf nanowhisker is somehow incompatible with MMT, causing agglomeration, load cannot be transferred effectively and thus tensile strength decreased. When 1 phr of MMT was added, 2 phr of kenaf increased the tensile strength but when 3 phr of MMT loading was added, 2 phr of kenaf decreased the tensile strength instead. At higher MMT loading, the incompatible kenaf nanowhisker and MMT tend to agglomerate more easily as there is increasing amount of particles in the matrix. Although both MMT and kenaf nanowhisker have hydroxyl group, the organic-inorganic hydrogen bonding between kenaf nanowhisker is very weak which gives no reinforcing effects to the polymer matrix (Darder, Colilla and Ruiz-Hitzky, 2003). Agglomeration causes PVOH not to form hydrogen bonds, either intermolecularly with nanowhisker or intramolecularly within PVOH

matrix itself to the extent that the nanocomposites cannot provide good tensile strength.

When the amount of MMT was fixed at 5 phr, the tensile strength trend was different from the tensile strength trend of 1 phr and 3 phr of MMT. The tensile strength first decreased at 2 phr, and then increased before decreased again at 8 phr of kenaf nanowhisker. MMT is nanoclay particle, which can attach well to the PVOH matrix by forming hydroxyl bonding. The higher the amount of MMT added, the higher the tensile strength of the nanocomposites (Tee, et al., 2013). Therefore, the reduced tensile strength due to agglomeration of kenaf nanowhisker might be counter balance by the enhanced mechanical properties of MMT at high MMT loading.

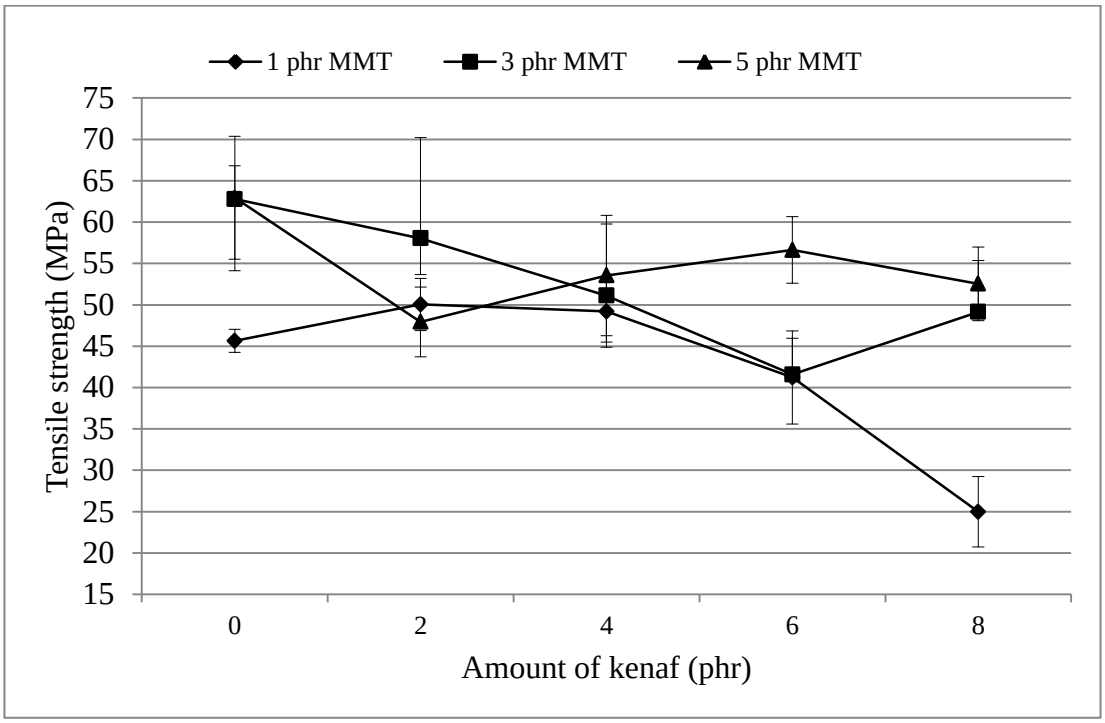

Figure 4.1: Tensile Strength of PVOH - Kenaf Nanowhisker - MMT nanocomposites with Fixed MMT Loading

Figure 4.2 shows the tensile strength of PVOH-kenaf nanowhisker-MMT nanocomposites with constant kenaf nanowhisker loading. Overall, the tensile strength has increasing trend. The tensile strength increased with increasing MMT loading except for nanocomposites with 2 phr of kenaf nanowhisker.

At fixed kenaf nanowhisker loading, as amount of MMT added increased, the tensile strength increased as well due to well development of polymer/clay nanocomposites. MMT is attached efficiently onto the PVOH matrix. Good interaction between PVOH matrix and MMT attributed to the homogeneous dispersion of the nano-sized MMT in PVOH matrix results in good interfacial interaction.

However, for kenaf nanowhisker loading at 2 phr, the tensile strength increased for 1 phr to 3 phr, then level off at 5 phr of MMT. The reduction of tensile strength is explained by the uneven distribution of the MMT particles during sample preparation. During solution casting, pouring of the solution of nanocomposites into petri dishes is one of the factors affecting the distribution of the MMT particles. When the solution was left still for longer time, the MMT and kenaf whisker started to sediment, causing uneven distribution of the MMT and nanowhisker particles when the solution was poured into petri dishes. Some regions have more MMT while some regions have lesser. The regions with lesser MMT have lower tensile strength as the reinforcing effect of MMT is lower. This nanocomposites is said to have lower loading of MMT than expected.

In addition, without addition of kenaf nanowhisker, which is at 0 phr of kenaf nanowhisker, the tensile strength increases drastically from 0 phr to 3 phr of kenaf nanowhisker added, then stay constant from 3 phr to 5 phr. This may due to there is a maximum tensile strength that can achieve when various amount of MMT is added. With addition of 3 phr and 5 phr of MMT, the maximum tensile strength has reached, indicating that further addition of higher MMT concentration will shows a decrease in tensile strength. This result was similar reported by Tee, et al., 2013 where the tensile strength started to decrease when more than 5 phr of MMT was added.

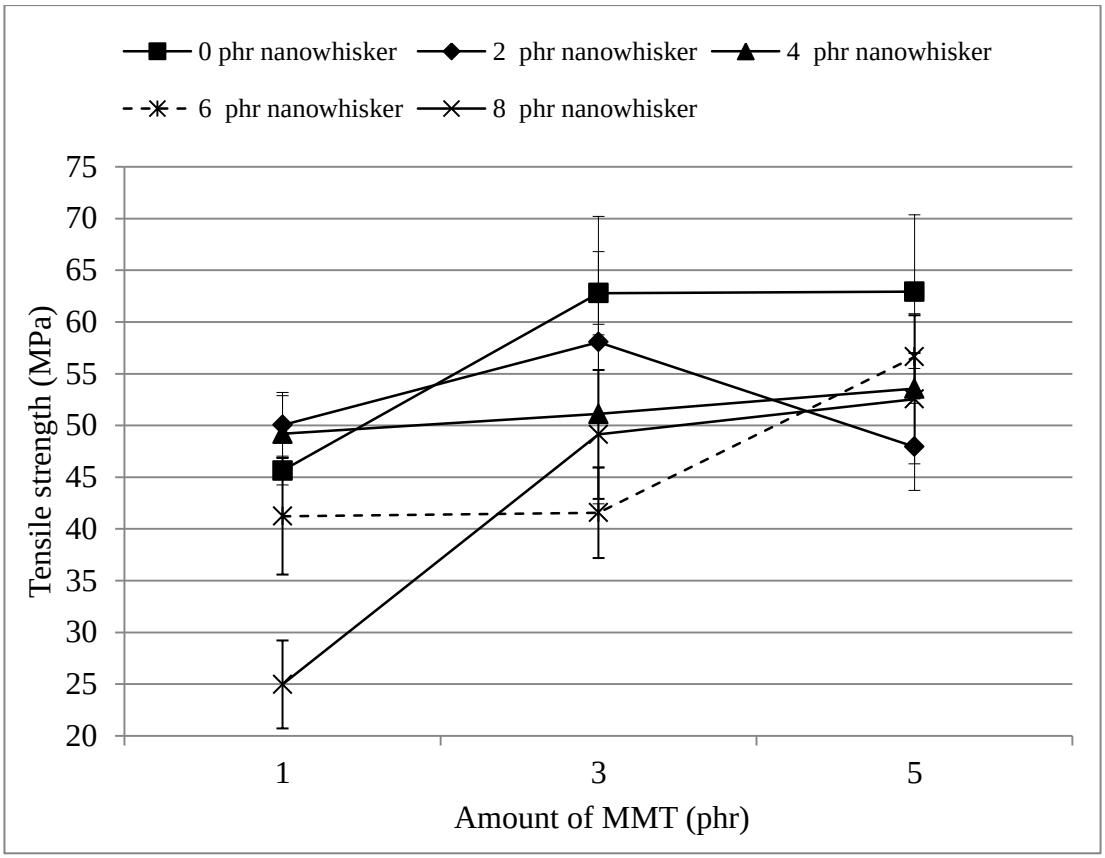

Figure 4.2: Tensile Strength of PVOH - Kenaf Nanowhisker - MMT Nanocomposites with Fixed Kenaf Nanowhisker Loading

4.1.2 Elongation at break

From Figure 4.3 shows the percentage elongation at break for PVOH-kenaf nanowhisker-MMT nanocomposites at constant MMT loading. The overall percentage elongation at break decreases with increasing kenaf nanowhisker loading although there is some point where the elongation is increasing.

When 1 phr of MMT was added with various amount of kenaf nanowhisker into PVOH matrix, the percentage of elongation at break graph shows a down and up trend. At the beginning, the elongation decreased drastically from 15.5 % to 5%, and then increases slightly to 6 %, beyond that which drops to less than 2%. PVOH itself has higher elongation at break due to its hydrophilic properties and ability to absorb water. Water will act as plasticizer to promote chain sliding, thus pure PVOH has

high elongation. When no kenaf nanowhisker was added, the elongation at break is extremely high compared to other nanocomposites. This value is similar reported by Tee, et al., 2013 where the PVOH added with 1 phr of MMT has elongation of about 23%. This is due to low concentration of additives (1 phr of MMT) does not give any significant effect to elongation of pure PVOH When the loading of kenaf nanowhisker was increasing from 0 phr to 8 phr, the factors that decreasing the elongation become significant, causing the elongation drops drastically. This is due to kenaf nanowhisker act as stress concentrator where all the stress applied will be transferred to kenaf nanowhisker particles. Thus, elongation decreased as the kenaf nanowhisker particles which take the high stress breaks faster. Besides that, the kenaf nanowhisker can form rigid network with the matrix, constraining the sliding and motion between polymer chains. Aggregation of kenaf nanowhisker particles is another factor decreasing the elongation at break. When the loading of kenaf nanowhisker increases, aggregation occurs due to uneven distribution. Aggregation creates more regions with high stress concentrator which contributes to lower elongation.

For 3 phr of MMT and 5 phr of MMT loading, the elongation increased at the beginning, then drop off after some point. The elongation at break level off at 2 phr of kenaf nanowhisker for 3 phr of MMT and level off at 4 phr of kenaf nanowhisker for 5 phr of MMT. These results are quite similar to that of 1 phr MMT loading except that for 3 MMT and 5 MMT loading do not experience a sharp decrease at the beginning. At low kenaf nanowhisker loading, increasing kenaf nanowhisker loading causes increment of elongation. This can be explained by the kenaf nanowhisker is water favourable due to its hydrophilic properties. Kenaf nanowhisker which acts as a good carrier of water somehow will increase the water content in nanocomposites, increases ductility of the nanocomposites and eventually increases the elongation at break. However, the elongation began to drop at certain concentration indicating agglomeration was occurring. For 3 phr of MMT, the elongation drops when more than 3 phr of kenaf nanowhisker was added while for 5 phr of MMT, the elongation drops when more than 2 phr of kenaf nanowhisker was added.

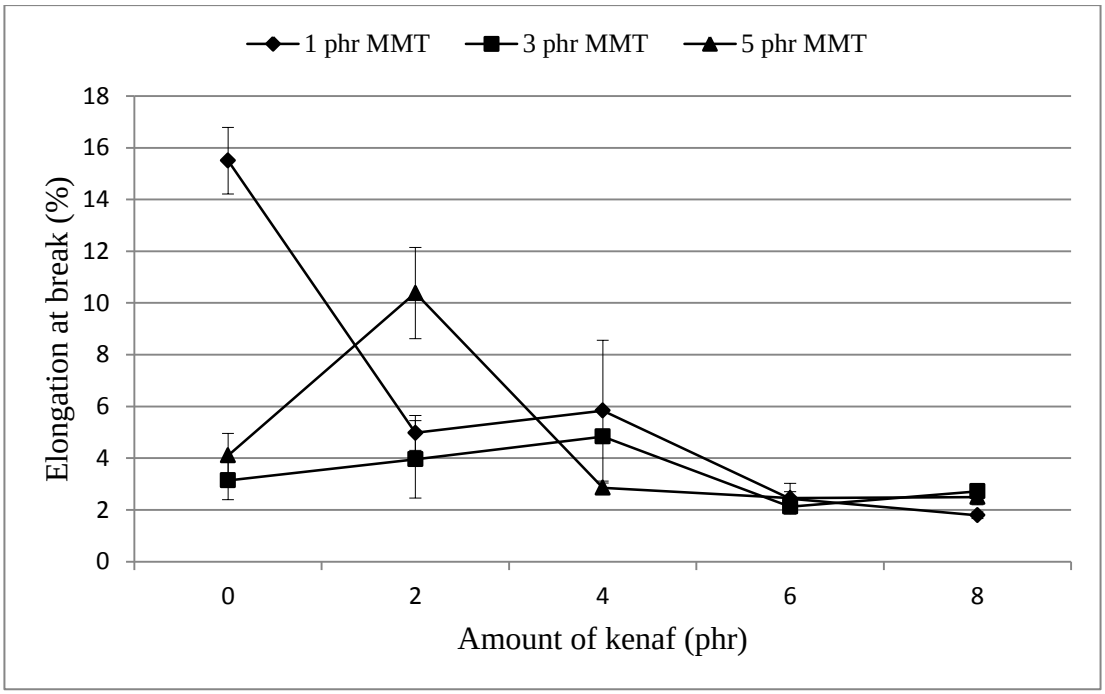

Figure 4.3: Elongation at Break of PVOH-Kenaf Nanowhisker-MMT Nanocomposites with Fixed MMT Loading

Figure 4.4 shows the percentage elongation at break for various amount of MMT added with fixed kenaf nanowhisker content. Generally, the elongation decreased with increasing of MMT loading. This can be explained by the MMT act as stress concentrator which in this case, MMT has same properties as kenaf nanowhisker, increasing region of high stress concentration in the polymer matrix. Incorporation of MMT in the PVOH matrix increases the brittleness of the nanocomposites, results in the fractures of the composite surface which contribute to the decreasing of elongation at break. In addition, further increment of MMT into PVOH matrix would causes agglomeration of MMT, forming irregular matrix chain that restrict recrystallization during deformation (Tee, et al., 2013), thus breaking point is reached at lower strain.

At 2 phr of kenaf nanowhisker and 5 phr of MMT loading, the elongation has a sudden increment. This increment is due to the uneven distribution of MMT in the PVOH matrix. This has been explained in section earlier where the nanocomposite with 2 phr of kenaf nanowhisker and 5 phr of MMT has lower tensile strength. The lower concentration of MMT contributed to higher elongation. As can be seen in

Figure 4.4, the elongation of nanocomposite with 5 phr of MMT is higher than nanocomposite with 3 phr of MMT but lower than nanocomposite with 1 phr of MMT. This means that the "actual" content of MMT is between 1 phr and 3 phr of MMT.

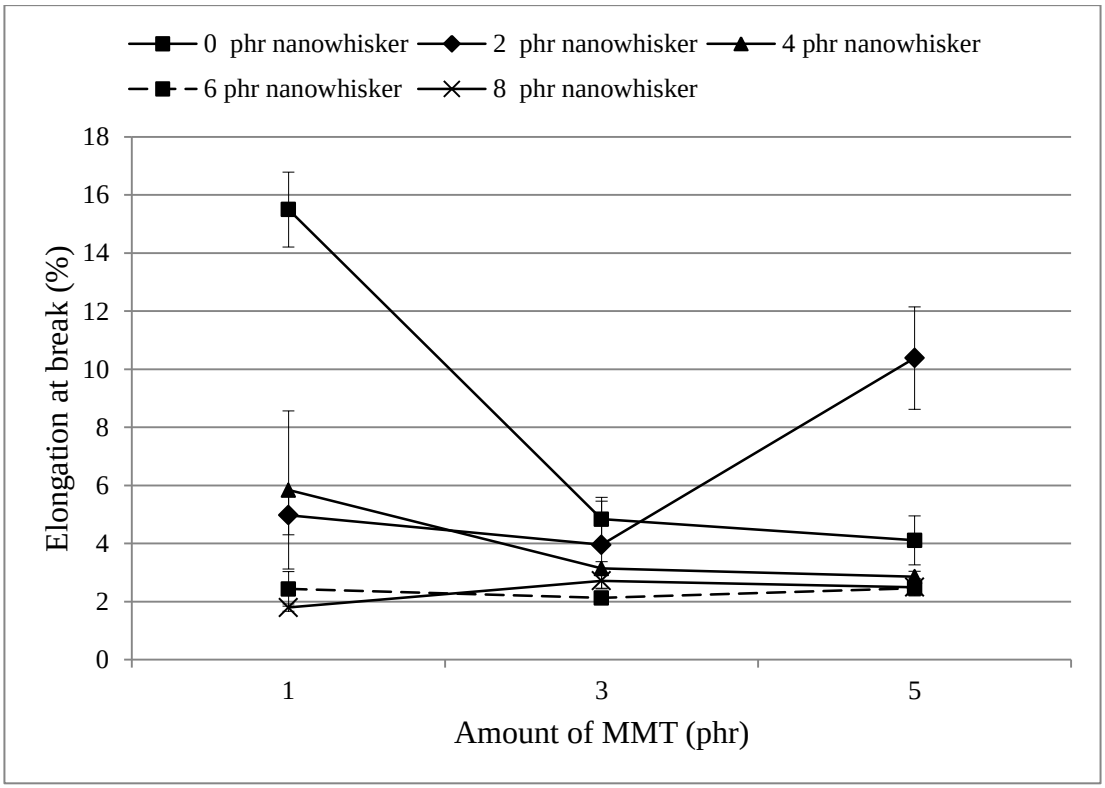

Figure 4.4: Elongation at Break of PVOH-Kenaf Nanowhisker-MMT Nanocomposites with Fixed Kenaf Nanowhisker Loading

4.1.3 Modulus

Figure 4.5 shows the modulus PVOH-kenaf nanowhisker-MMT nanocomposite with constant MMT loading. As can be seen from Figure 4.5, the modulus of various kenaf nanowhisker loading incorporated with fixed amount of MMT has no fixed trend. For 1 phr of MMT, the increasing kenaf nanowhisker loading decreased the modulus at low kenaf nanowhisker loading, and the modulus started to increase when more than 4 phr of kenaf nanowhisker is added while for 3 phr and 5 phr of MMT,

the modulus increased until 4 phr of kenaf nanowhisker, beyond that which the modulus decreased.

For 1 phr of MMT added, the modulus first decreased slightly due to low content of kenaf nanowhisker does not give significant effect on reinforcing. When the kenaf nanowhisker loading is more than 4 phr, it started to provide reinforcement for the nanocomposites. The increasing of modulus was attributed by the reinforcement of the stronger kenaf nanowhisker. Due to extensive intramolecular and intermolecular hydrogen bonding within nanocellulose itself, kenaf nanowhisker has stiffer and more rigid chain than PVOH, thus increasing its nanocomposites' modulus. Furthermore, homogeneous dispersion and the good surface interaction between kenaf nanowhisker and PVOH also contribute to high modulus.

For 3 phr and 5 phr of MMT, the increasing trend is different from the decreasing trend for 1 phr of MMT. This might be due to only high MMT content can promote the reinforcing force of kenaf nanowhisker. Beyond loading of 4 phr of kenaf nanowhisker, agglomeration happens, causes the interfacial adhesion and surface interaction between kenaf nanowhisker and PVOH become weaker, thus decreasing the modulus at high kenaf nanowhisker content.

As can be seen from Figure 4.5 below, the standard deviation is large as compared to tensile strength and elongation graphs. Uneven dispersion of the kenaf nanowhisker and MMT particles is one of the reasons attributed to such a high standard deviation.

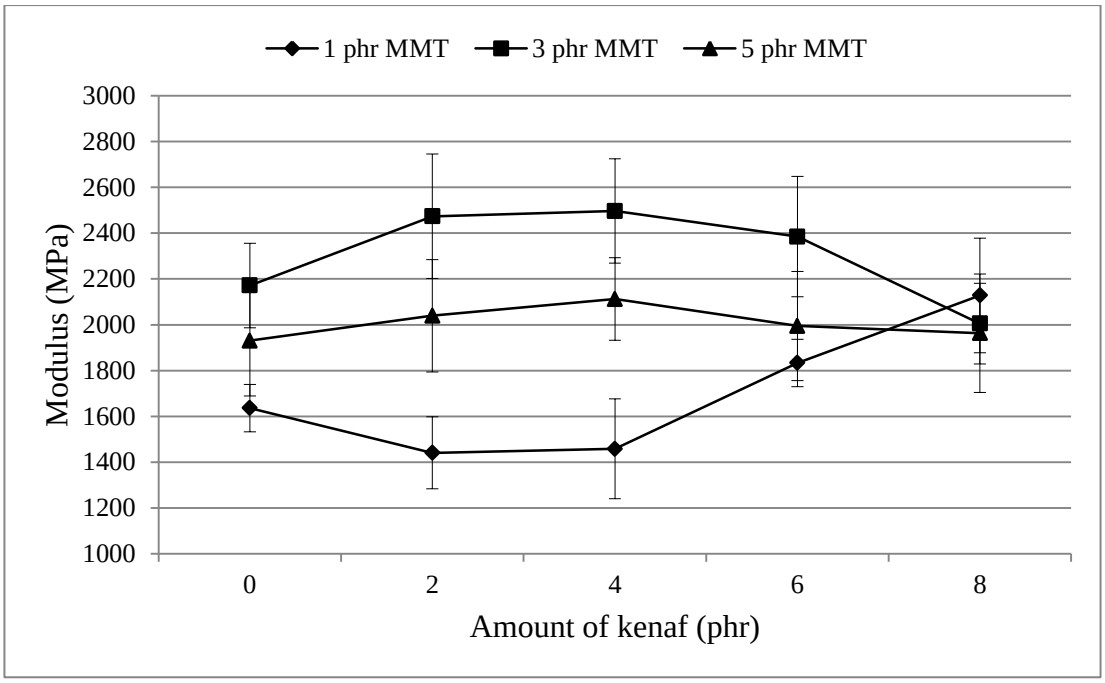

Figure 4.5: Young's Modulus of PVOH-Kenaf Nanowhisker-MMT Nanocomposites with Fixed MMT Loading

Figure 4.6 below shows the modulus PVOH-kenaf nanowhisker-MMT nanocomposite with constant kenaf nanowhisker loading. Most of the modulus line increased until a certain level, then level off except for nanocomposites at 4 phr and 8 phr of kenaf nanowhisker.

Initially, the increasing modulus is due to the good interaction between MMT layers and PVOH matrix. Forming of hydrogen bonds between MMT and PVOH indicates that there is a good interfacial adhesion. Besides, MMT incorporated into PVOH matrix can restricts the polymer chain motion (Velmurugan and Mohan, 2009). Therefore, high stress and low strain results in high modulus value. Later, the decreasing modulus might due to agglomeration of MMT at high MMT loading. As the MMT loading increases, MMT particles tend to form hydrogen bonds within itself. This self-aggregation cause the aspect ratio of MMT decrease, results in poor interfacial adhesion. Thus, the modulus decreases.

At 8 phr of kenaf nanowhisker, the modulus decreased with increment of MMT loading. 8 phr of kenaf nanowhisker is considered as high concentration.

When such a high concentration is present in the PVOH matrix, agglomeration occurs easily as more particles are competing with each other to form hydrogen bonds with the polymer matrix. MMT cannot have a good surface interaction with the polymer matrix, thus the modulus value is declining.

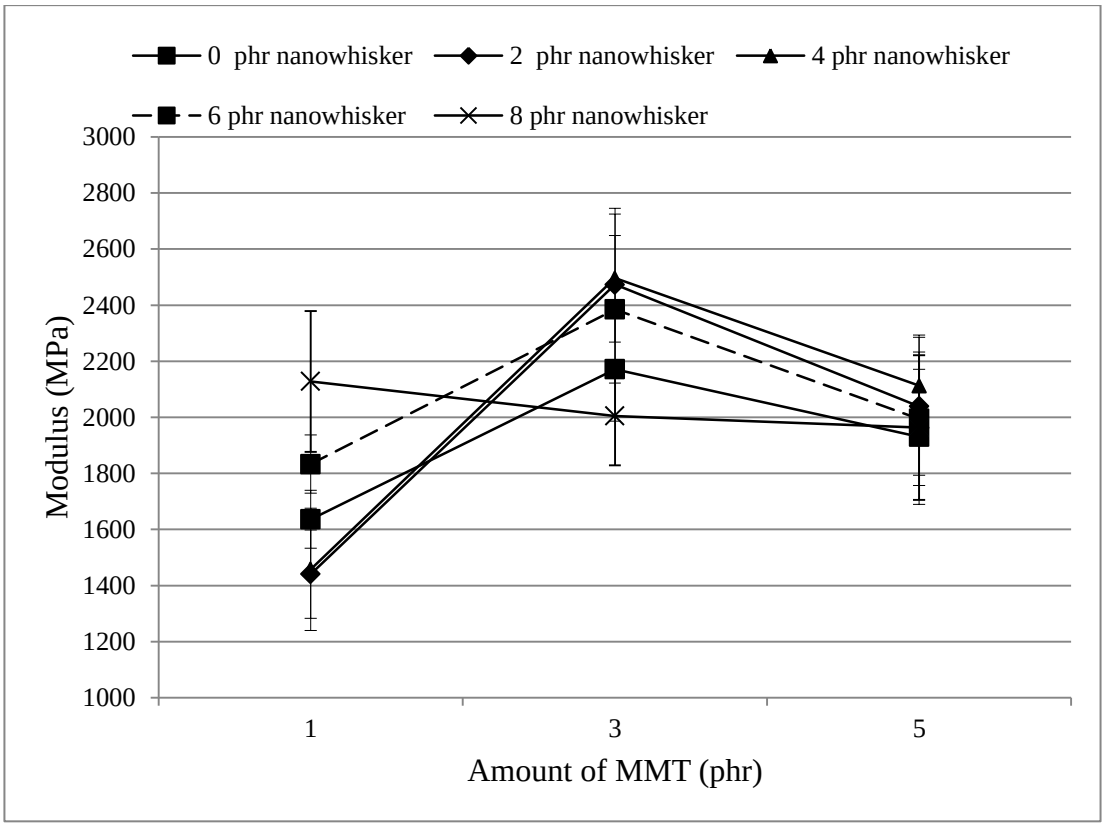

Figure 4.6: Young's Modulus of PVOH-Kenaf Nanowhisker-MMT Nanocomposites with Fixed Kenaf Nanowhisker Loading

4.2 Differential Scanning Calorimetry (DSC)

4.2.1 Peak heating temperature of PVOH-kenaf nanowhisker-MMT nanocomposites

In this study, DSC thermograms were used to determine the peak heating behaviour of the PVOH-kenaf nanowhisker-MMT nanocomposites. The analysis was done mainly focus on the maximum heating temperature corresponding to the lowest peak in DSC thermogram. Indeed, this is not the melting temperature to melt the nanocomposites. This peak heating peak is corresponding to the temperature that needed to enable vibration of amorphous region of the nanocomposites.

Figure 4.7 shows the DSC thermograms for nanocomposites with 1 phr of MMT and various amount of kenaf nanowhisker. When 1 phr of MMT was incorporated with increasing amount of kenaf nanowhisker into PVOH, the peak heating temperature decreased slightly from 0 phr to 2 phr of kenaf nanowhisker, then increased for 4 phr to 6 phr, and lastly decreased when 8 phr of kenaf nanowhisker was added. As can be clearly seen from Figure 4.10, the highest heating temperature for nanocomposites with 1 phr of MMT is 124.94 °C, when 6 phr of kenaf nanowhisker were incorporated into PVOH matrix. The increasing trend from 2 phr to 6 phr might be explained by the addition of kenaf nanowhisker and MMT have good interaction with the PVOH matrix and provide interactive effect towards highly stable structure (Lee, et al., 2010). Kenaf nanowhisker and MMT both containing hydrogen bonds that formed hydrogen bonds with PVOH, forming a higher rigidity of matrix, thus more energy is needed to vibrate the stronger hydrogen bonding. In another word, higher heating temperature is achieved to provide higher amount of heat to cause vibration to the high energy stability system. At higher kenaf nanowhisker loading, the kenaf nanowhisker has tendency to agglomerate due to uneven distribution of the particles. Agglomeration contributes to weaker interfacial adhesion and thus weaker hydrogen bonding. Furthermore, agglomeration can cause the regular chain of PVOH matrix to become irregular chain arrangement that subsequently reducing the existing hydrogen bonding strength within polymer matrix. This explained why the peak heating temperature decreased when 8 phr of kenaf nanowhisker was added and the peak heating temperature was even lower than

nanocomposites with no addition of kenaf nanowhisker. This can be used to further support the tensile strength where kenaf nanowhisker particles tend to agglomerate in PVOH matrix and reduced the tensile strength at high nanowhisker loading.

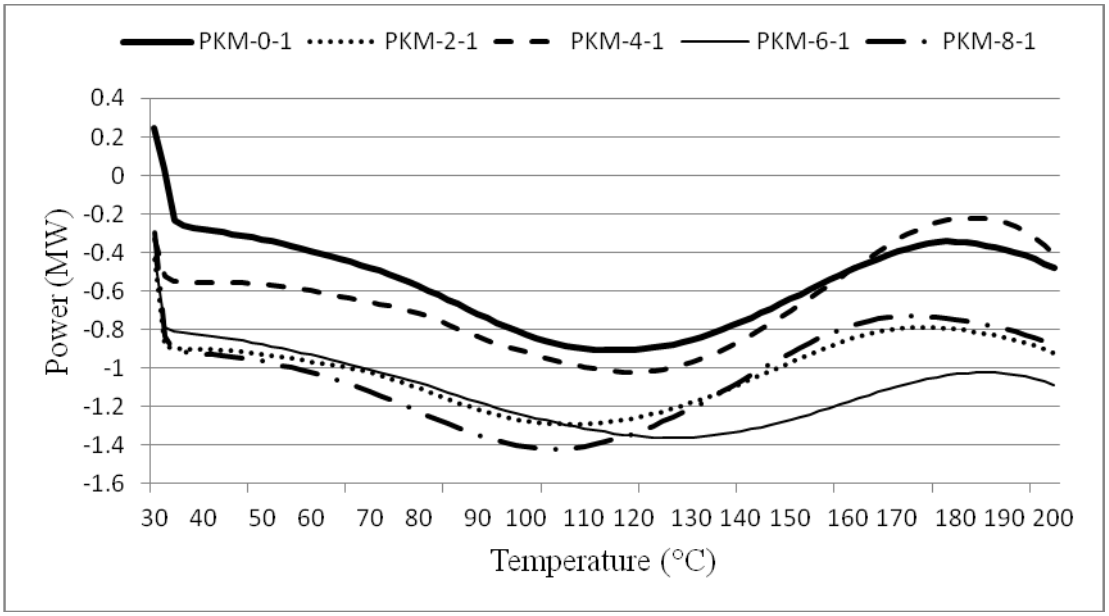

Figure 4.7: DSC Thermograms for 1 phr of MMT and Various Amount of Kenaf Nanowhisker

Figure 4.9 shows the DSC thermograms for nanocomposites with 5 phr of MMT and various amount of kenaf nanowhisker. When 5 phr of MMT was incorporated with various amount of kenaf nanowhisker into PVOH, the DSC thermograms showed the same trend as above. However, for 3 phr of MMT incorporated with various amount of kenaf nanowhisker into PVOH, the DSC thermograms showed a different trend as shown in Figure 4.8. The peak heating temperature first increased for 0 phr to 2 phr, then decreased for 4 phr to 6 phr, and lastly increased when 8 phr of kenaf nanowhisker was added. The first increasing trend is attributed by the good surface interaction between kenaf nanowhisker and MMT, forming strong hydrogen bonding. At 4 phr and 6 phr of kenaf nanowhisker added, agglomeration started to occur where hydrogen bonding become lesser and weaker, disturbed the regular chain of matrix causing heat temperature decreased. Nevertheless, the peak heating temperature increased when 8 phr of kenaf nanowhisker and 3 phr of MMT were added. This might be due to high concentration

of kenaf nanowhisker and MMT, these large numbers of nano-sized particles can be distributed in every corner and forming hydrogen bonds with PVOH matrix although agglomeration still occurs. The superior effect of forming large number of hydrogen bonding might dominant over the inferior effect of agglomeration. Therefore, the heat temperature has increased.

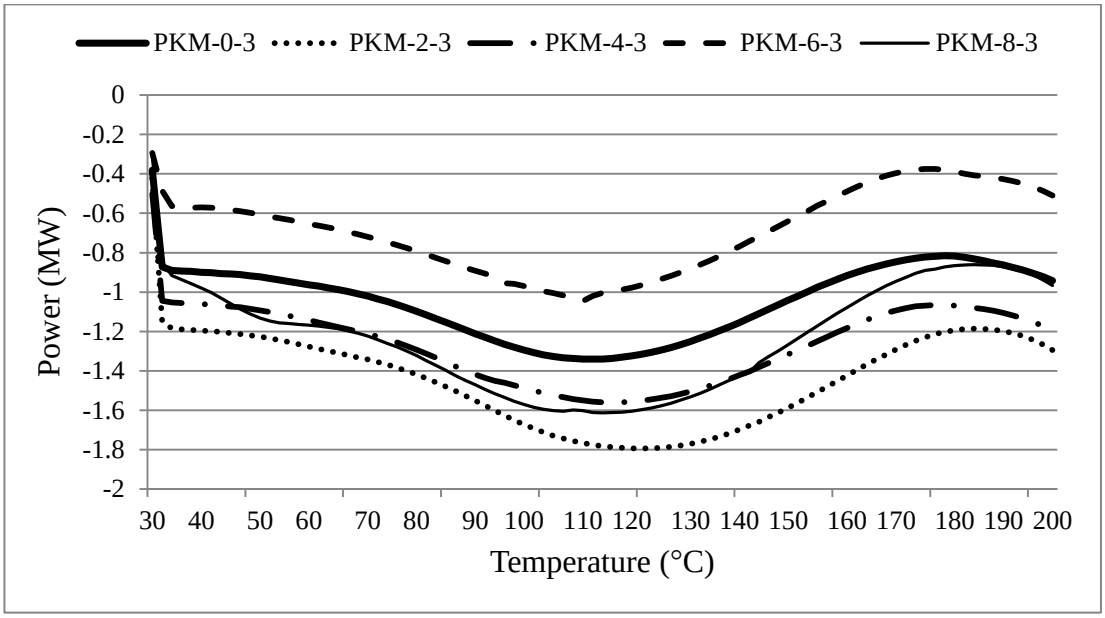

Figure 4.8: DSC Thermograms for 3 phr of MMT and Various Amount of Kenaf Nanowhisker

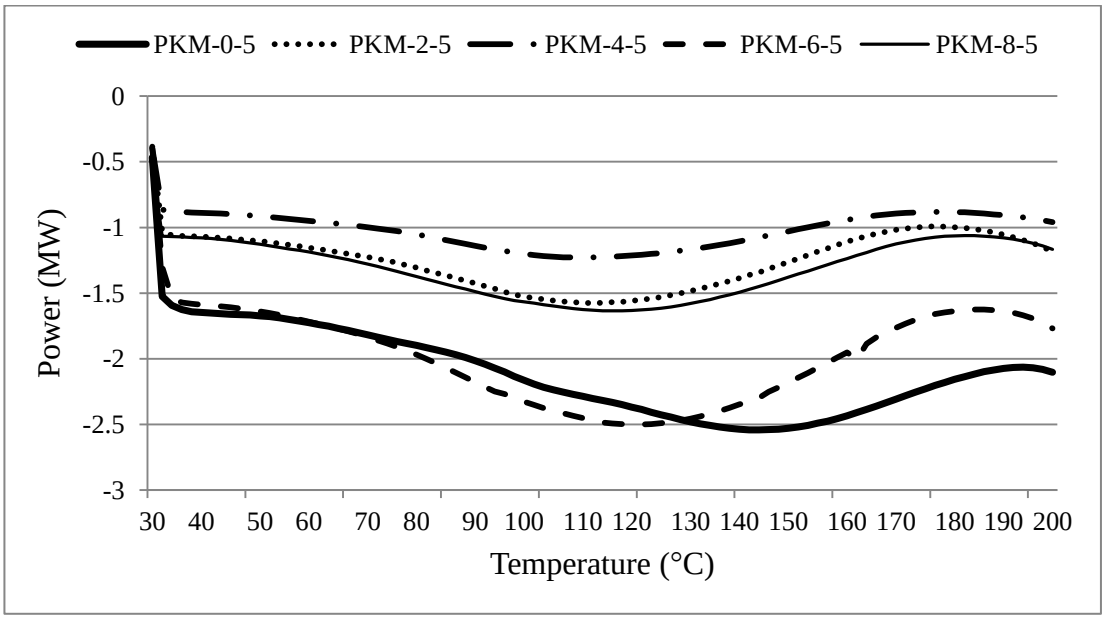

Figure 4.9: DSC Thermograms for 5 phr of MMT and Various Amount of Kenaf Nanowhisker

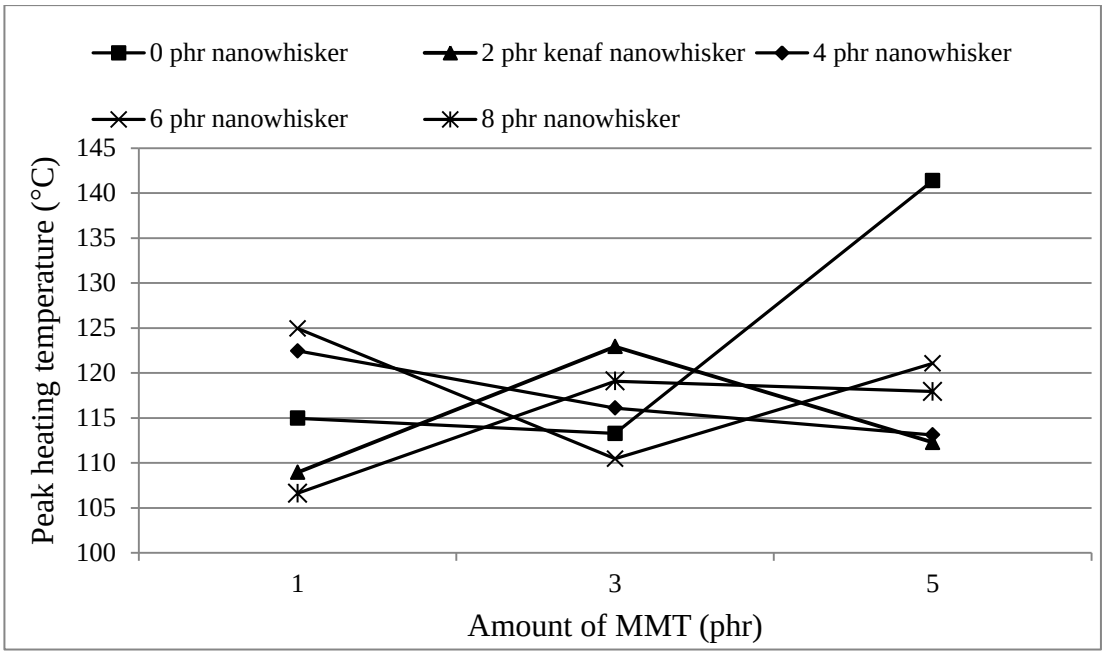

Figure 4.10: Peak Heating Temperatures for PVOH-Kenaf Nanowhisker-MMT Nanocomposites

4.3 Scanning Electron Microscopy (SEM)

4.3.1 Interaction of PVOH-MMT with various amount of kenaf nanowhisker

Figure 4.11 below shows the surface morphology for PVOH incorporated with 1 phr of MMT and various amount of kenaf nanowhisker. It can be seen that by comparing Figure 4.11 from (a) to (e), the surface became rough with increment of kenaf nanowhisker content. At low kenaf nanowhisker 4 phr loading, the PVOH has exhibited as a continuous matrix. This was attributed by the well dispersion of kenaf nanowhisker and MMT at low content, thus no MMT and kenaf nanowhisker can be seen as their nano-sized particles are too small. Strong hydrogen bonding can resist tearing effect by extending the continuity of chain (Gad, 2009). When stress was applied, the nanocomposites breaks in an ordered way along throughout the matrix, indicates effective load transfer. Evenly distribution of the kenaf nanowhisker and MMT contributed to good interfacial adhesion between each other, providing effective load transfer system which enable matrix to elongate more when stress is applied. This good reinforcing effect eventually provides high tensile strength and elongation at break.

However, the superior effect is only limited up to a composition where upon the maximum point, the system acts in a different manner. As the amount of kenaf nanowhisker increases to 6 phr, agglomeration of kenaf nanowhisker started to occur as shown by the white spots and the matrix shows less continuity. Kenaf nanowhisker prefers to form hydrogen bond within itself rather than with PVOH, causing agglomeration occurred. Kenaf nanowhisker has a tendency to have phase separation and pass through the surface in the form of bright globular surface (Mandal and Chakrabarty, 2014). Agglomeration was occurred due to the poor distribution of kenaf nanowhisker in polymer matrix, leading to poor interfacial adhesion. Applied stress cannot be transferred effectively throughout the matrix and causing all the stress concentrates at the agglomeration point. This is the reason for reduction of tensile strength and elongation when high loading of kenaf nanowhisker was added. When 8 phr of nanowhisker was added, agglomeration became more severe as flakes-like structure was observed in Figure 4.11 (e). Existing of flakes-like structure indicates that the matrix continuity reduced, nanocomposites became more

brittle, as a result the nanocomposites break faster when stress was applied, and further decreased the tensile strength and elongation.

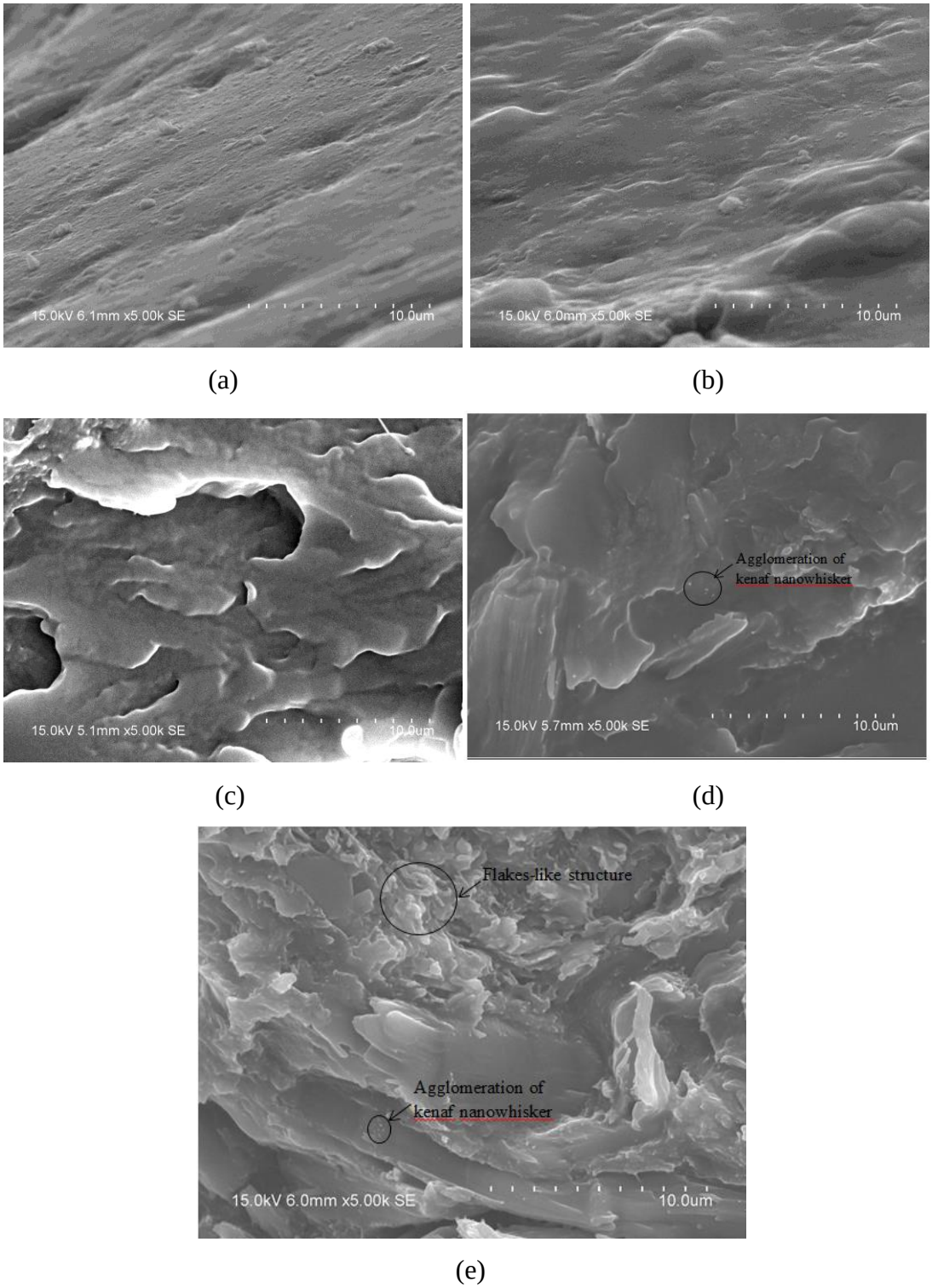

Figure 4.11: SEM of 1 phr of MMT Incorporated into PVOH Added with (a) 0 phr Nanowhisker; (b) 2 phr Nanowhisker; (c) 4 phr Nanowhisker; (d) 6 phr Nanowhisker; (e) 8 phr Nanowhisker

4.3.2 Interaction of PVOH-MMT with various amount of MMT

Figure 4.12 below shows the surface morphology for PVOH incorporated with 8 phr of kenaf nanowhisker and various amount of MMT. When MMT loading increasing from 1 phr to 3 phr, it can be seen that the MMT was distributed evenly in PVOH matrix as no MMT particles can be seen from the Figure. This indicates that MMT formed hydrogen bonding with PVOH matrix contributed to good interfacial adhesion of MMT and thus good dispersion within PVOH matrix. The matrix has high continuity and good tearing effect resistant contributed to high elongation at break.

However, when 5 phr of MMT was added, flakes-like structure was observed. This flakes-like structure might due to the formation of aggregates by MMT and kenaf nanowhisker. This resulted in decrease in elongation at break as flakes-like structure cannot transfer load effectively, forming stress concentrator region, increase the brittleness and causing the nanocomposite breaks faster when high stress was applied. Yet, the tensile strength of 5 phr MMT was slightly higher compared to 3 phr MMT. This is because only slight aggregation was formed where the effect is not significant. As shown in Figure 4.12 (c), only small part of the matrix actually having the flakes-like structure, where most of the matrix still remains in continuity form. Furthermore, MMT exhibits better tensile properties through its interaction with PVOH matrix. This superior properties was overriding the inferior properties, thus the tensile strength was higher.

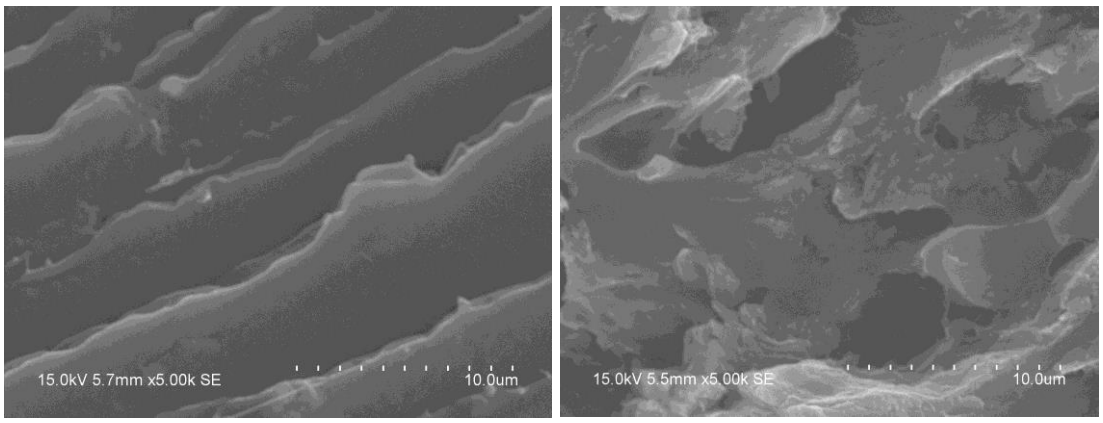

(a) (b)

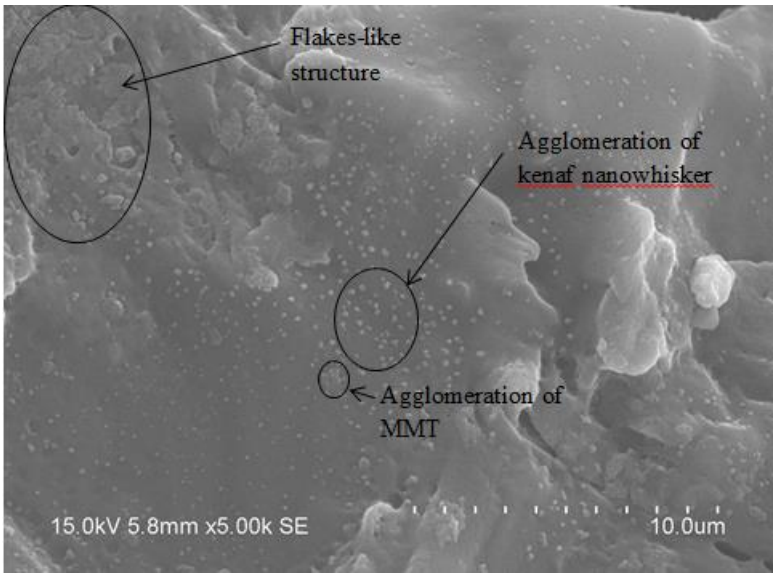

(c)

Figure 4.12: SEM of 8 phr of Kenaf Nanowhisker Incorporated Into PVOH Added with (a) 1 phr MMT; (b) 3 phr MMT; (c) 5 phr MMT

4.4 X-ray Diffraction (XRD)

4.4.1 Crystallite size

Figure 4.13 below shows the XRD patterns for PVOH incorporated with 6 phr of kenaf nanowhisker and various amount of MMT. PVOH exhibited 5 obvious peaks (shown as peak A, peak B, peak C, peak E and peak F). Peak D of pure PVOH is too low, not obvious to be seen as compared to nanocomposites. However, when kenaf nanowhisker and MMT were added into PVOH, the nanocomposites exhibited 6 obvious peaks (shown as peak A, peak B, peak C, peak D, peak D, peak E and peak F). Peak D became obvious when kenaf nanowhisker and MMT were added. This might due to the formation of new crystallite structure induced by kenaf nanowhisker. Kenaf nanowhisker has formed new hydrogen bonding with polymer matrix as both are hydrophilic and contains hydroxyl groups, promote to an order chain arrangement, and thus induces formation of new crystallites. Among all, peak F was the sharpest, indicates that the crystallite structure of peak F has the largest size. Addition of kenaf nanowhisker and MMT has no inferior effect on the sharpness of peak F, instead increased its intensity, point toward the good interaction between PVOH, kenaf nanowhisker and MMT, increasing the crystallinity of the crystallite. Besides, Peak A and E also have the almost same broadness as pure PVOH.

However, kenaf nanowhisker and MMT have broadened the peak B and peak C. This shows that the crystallite size at peak B and C is reduced due to poor interaction between kenaf nanowhisker and MMT with PVOH matrix, as well as the addition of kenaf nanowhisker and MMT have interrupted and disturbed the bonding of PVOH. The regularity of matrix chain arrangement is reduced, crystal starts to rupture, causing crystallite size decreased, eventually could change the structure from crystallite to amorphous and reduce the crystallinity.

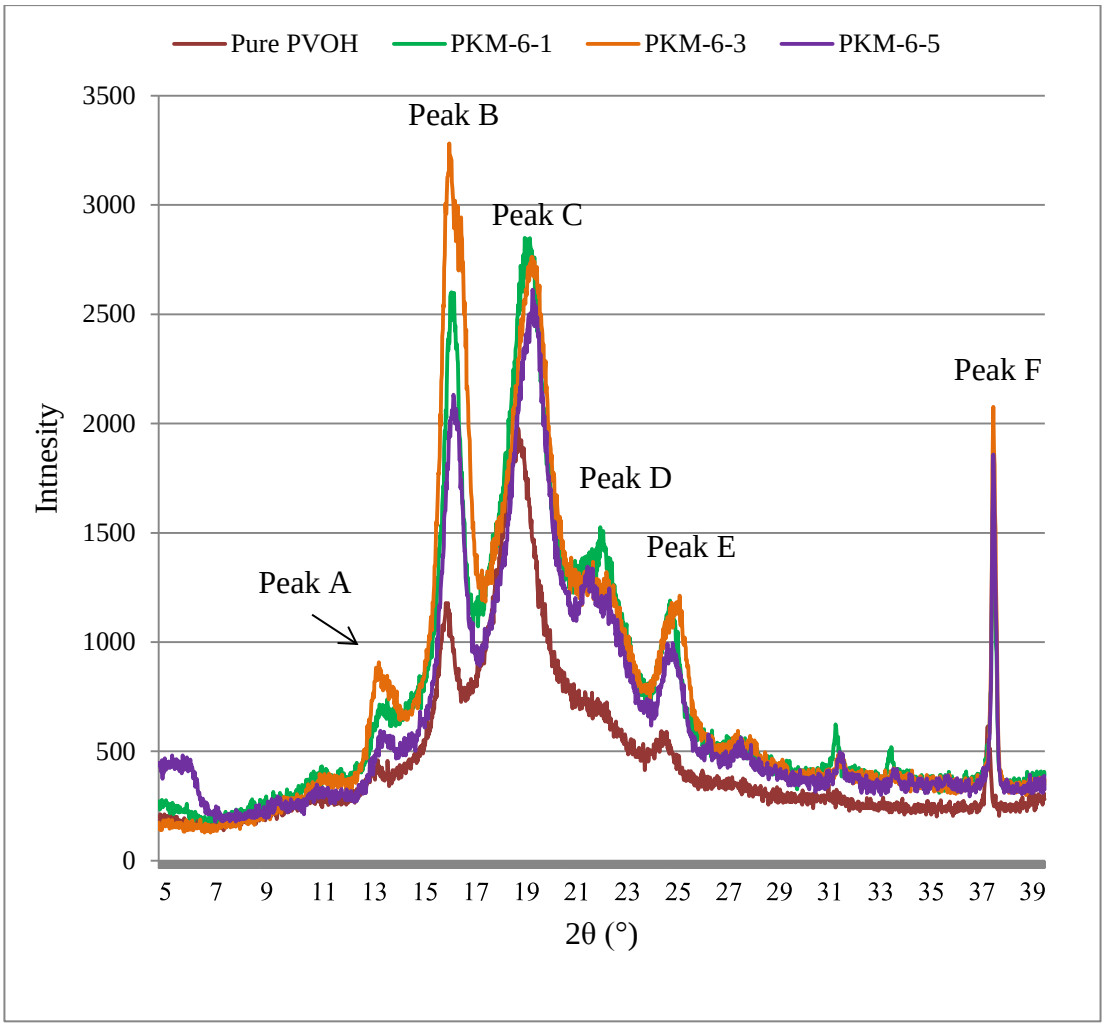

Figure 4.13: XRD Curves for Pure PVOH and PVOH Added with 6 phr of Kenaf Nanowhisker and Various Amount of MMT

Figure 4.14 below shows the XRD patterns for PVOH incorporated with 8 phr of kenaf nanowhisker and various amount of MMT. The nanocomposites exhibited 6 obvious peaks (shown as peak A, peak B, peak C, peak D, peak E and peak F). However, peak D of nanocomposites with 8 phr of kenaf nanowhisker is too low, not obvious to be seen as compared to nanocomposites with 6 phr of kenaf nanowhisker. This shows that at low kenaf nanowhisker content (6 phr), the kenaf nanowhisker interacts well with PVOH matrix, induced formation of new crystallite structure with high intensity. However, at high kenaf nanowhisker content (8 phr), the kenaf nanowhisker does not shows reinforcing effect at peak D, no new crystallite is formed and thus no peak is found. This might due to at high kenaf nanowhisker content (8 phr), agglomeration occurs and causing the interfacial

adhesion decreases and no new bond is formed to induced formation of new crystallite structure.

When kenaf nanowhisker and MMT were added, no changes to the broadness of peak F. Peak A, B and E became broader when kenaf nanowhisker and MMT were added. Conversely, Peak C is sharpen when kenaf nanowhisker and MMT is added. The existing crystallite of PVOH matrix interacts with the newly bond by kenaf nanowhisker and MMT, forming bonding that could promote more ordered chain arrangement, thus induced new crystallite size of the crystal to a larger extent, subsequently sharpen the peak. At 6 phr of kenaf nanowhisker, there is no change of the broadness of peak A. Nevertheless, at 8 phr of kenaf nanowhisker, peak A became sharper. This shows that at low kenaf nanowhisker loading (6 phr), kenaf nanowhisker loading is too low to shows any reinforcing effect while at high kenaf nanowhisker loading (8 phr), kenaf nanowhisker starts to form bonding with existing crystallite, successively increase crystallite size and sharpen peak A which could greatly increase the crystallinity for 8 phr of kenaf nanowhisker content.

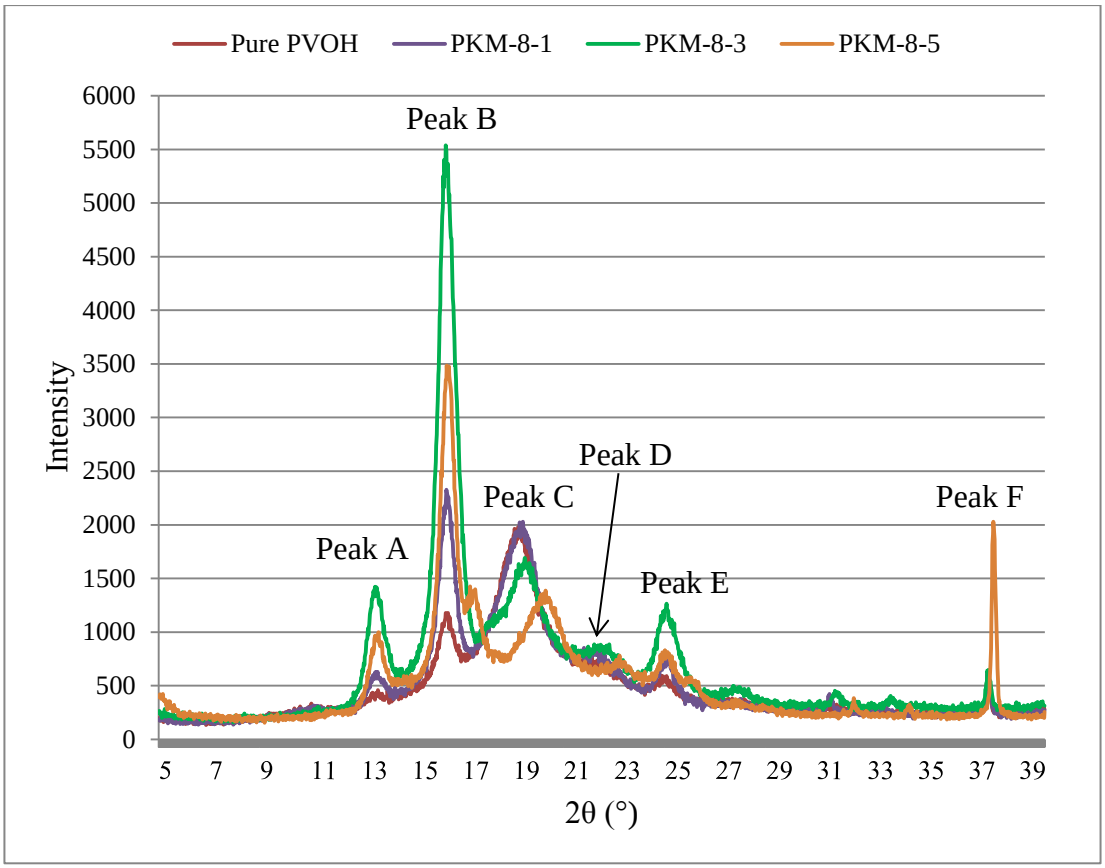

Figure 4.14: XRD Curves for Pure PVOH and PVOH Added with 8 phr of Kenaf Nanowhisker and Various Amount of MMT

4.4.2 Crystallinity

Figure 4.15 below shows the crystallinity for PVOH-kenaf nanowhisker-MMT nanocomposites. For 6 phr of kenaf nanowhisker loading, when the amount of MMT increased from 1 phr to 3 phr, the crystallinity increased from 12% to 13.7%, and when 5 phr of MMT was added, the crystallinity drops to 12%. This might be due to at low MMT loading, increasing amount of MMT will increased the interaction and hydrogen bonding with polymer matrix, inducing formation of more crystallite structures and thus crystallinity increased. At MMT loading higher than 3 phr, the MMT starts to agglomerate. Agglomeration will disturb and rupture the ordered chain arrangement of polymer matrix, thus decreases crystallinity. However, this increase and decrease of crystallinity is not significant as the difference is only about 1.7% of crystallinity.

For 8 phr of kenaf nanowhisker loading, when the amount of MMT increased from 1 phr to 5 phr, the crystallinity increased from 14% to 18.5%. High loading of kenaf nanowhisker might promote interaction with MMT, thus reducing MMT agglomeration. This result is tally with the tensile result where increasing MMT loading increased the tensile strength.

As can be seen from Figure 4.15 below, the overall crystallinity for 8 phr of kenaf nanowhisker is higher than the crystallinity for 6 phr of kenaf nanowhisker. This can be explained high kenaf nanowhisker loading has induced formation of more crystallite structure and promote bonding interaction of MMT with PVOH. Although high kenaf nanowhisker content might causes agglomeration, the superior effect of high kenaf nanowhisker loading is more significant than the inferior effect, thus the overall crystallinity increases.

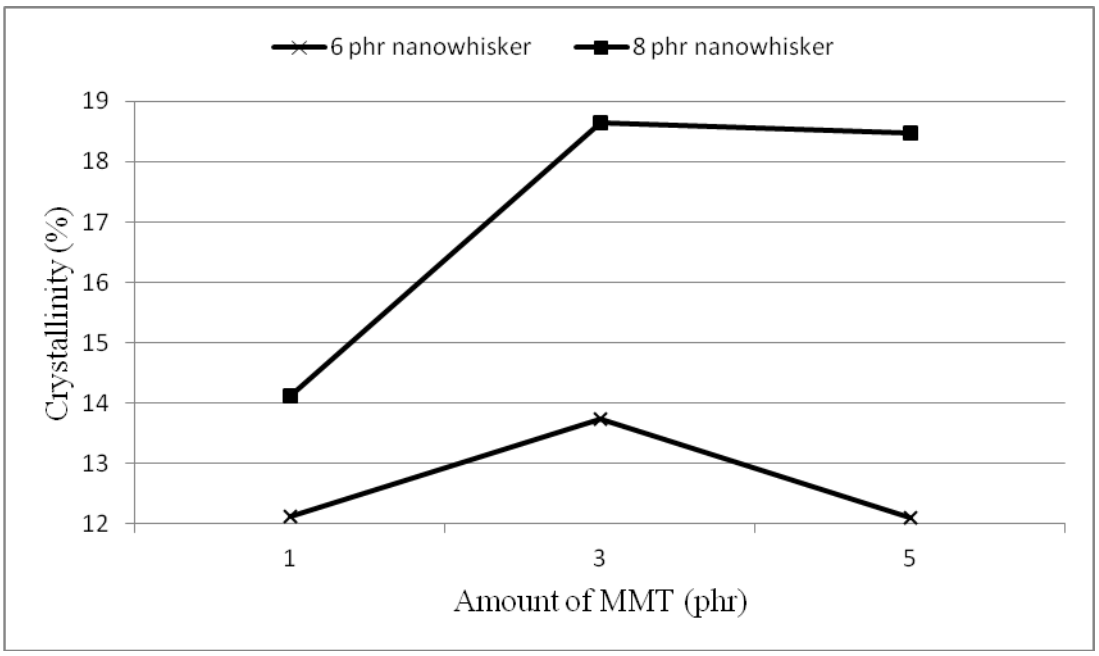

Figure 4.15: Crystallinity for PVOH-Kenaf Nanowhisker-MMT Nanocomposites

CHAPTER 5

CONCLUSION AND RECOMMENDATIONS

5.1 Conclusion

This study has evaluated the investigation of polyvinyl alcohol (PVOH) added kenaf nanowhisker and montmorillonite (MMT). Following are the conclusion made from this study:

5.1.1 Mechanical properties

For nanocomposites with 1 phr of MMT added, the tensile strength increased when 0 phr to 2 phr of kenaf nanowhisker was added, upon that the maximum point tensile strength decreased. For nanocomposites with 3 phr of MMT, the tensile strength decreased with increasing kenaf nanowhisker loading. For nanocomposites with 5 phr of MMT added, the tensile strength decreased when 0 phr to 2 phr of kenaf nanowhisker was added, then increased until a maximum at loading of 6 phr kenaf nanowhisker, upon that tensile strength decreased. For fixed amount of kenaf nanowhisker, the tensile strength increased with increasing MMT loading except for nanocomposites with 2 phr of kenaf nanowhisker where the maximum tensile strength occurred at 3 phr of MMT, upon that the tensile strength decreased

The elongation at break has the opposite trend with tensile. If tensile strength increased, the elongation decreased and vice-versa. However, at high kenaf

nanowhisker loading (6 phr and 8 phr), the elongation at break decreased to a very low value regardless of increasing or decreasing of the tensile strength.

The modulus of nanocomposites with fixed amount of kenaf nanowhisker were increased to a maximum point at 3 phr MMT loading, upon that the modulus decreased except for nanocomposites with 8 phr of kenaf nanowhisker where the modulus was decreased with increasing MMT loading. When the amount of MMT were fixed at 1 phr, the modulus decreased tp a lowest point at 4 phr of kenaf nanowhisker, and increased when more than 4 phr of kenaf nanowhisker were added. When the amount of MMT were fixed at 3 phr and 5 phr, the modulus increased until a maximum point at 4 phr of kenaf nanowhisker, and decreased when more than 4 phr of kenaf nanowhisker were added.

5.1.2 Thermal properties

Differential Scanning Calorimetry (DSC) shows the peak heating temperature of nanocomposites at amorphous state. When 1 phr and 5 phr of MMT was incorporated with increasing amount of kenaf nanowhisker into PVOH, the peak heating temperature decreased slightly when kenaf nanowhisker increased from 0 phr to 2 phr, then increased when kenaf nanowhisker increased from 2 phr to 6 phr, and lastly the peak heating temperature decreased again when 8 phr of kenaf nanowhisker was added. For 3 phr of MMT added, the peak heating temperature first increased when kenaf nanowhisker increased from 0 phr to 2 phr, then decreased when kenaf nanowhisker increased from 2 phr to 6 phr, and lastly the peak heating temperature increased when 8 phr of kenaf nanowhisker was added.

5.1.3 Microstructure

Scanning Electron Microscopy (SEM) result shows flakes-like structure was observed with increasing kenaf nanowhisker (from 0 phr to 8 phr) and MMT (from 1

phr to 5 phr) content which could reduce the elongation at break. At 1 phr of MMT, nanocomposites with kenaf nanowhisker content increasing from 0 phr to 4 phr had continuity matrix, showing high tensile strength whereas when kenaf nanowhisker content from 4 phr to 8 phr, agglomeration was observed which reduced the tensile strength. At 8 phr of kenaf nanowhisker, nanocomposites with MMT content increasing from 1 phr to 3 phr had continuity matrix thus tensile strength increased.

X-ray diffraction (XRD) result shows an increased in crystallinity of nanocomposites with increment of MMT content. For low kenaf nanowhisker content, when the amount of MMT increased from 1 phr to 3 phr, the crystallinity increased slightly from 12% to 13.7%, and when 5 phr of MMT was added, the crystallinity drops to 12%. For 8 phr of kenaf nanowhisker loading, when the amount of MMT increased from 1 phr to 5 phr, the crystallinity increased from 14% to 18.5%. New crystallite structure was formed when kenaf nanowhisker and MMT were added PVOH at around $2\theta = 22°$.

5.2 Recommendations

It is recommended that more analysis shall be carried out to provide more supportive evidence to conclude the properties of the PVOH-kenaf nanowhisker-MMT nanocomposites. Thermogravimetric analysis (TGA) shall be used to analyse the thermal stability of nanocomposites. Fourier Transform Infrared (FTIR) shall be used to analyse the bonding interaction in the nanocomposites.

Besides that, homogenous distribution of additives in PVOH matrix is one of the important factors affecting the properties of nanocomposites. Is it recommended that more care should be taken while stirring and casting the nanocomposites to avoid uneven dispersion. Impurities of raw materials must be reduced to minimum to increase purity of the samples.

REFERENCES

Aji, I., Sapuan, S., Zainudin, E. and Abdan, K., 2009. Kenaf fibres as reinforcement for polymeric composites: a review. International Journal of Mechanical and Materials Engineering, 4(3), pp. 239-248.

Akil, H., Omar, M., Mazuki, A., Safiee, S., Ishak, Z. and Abu Bakar, A., 2011. Kenaf fiber reinforced composites: A review. Materials & Design, 32(8), pp. 4107-4121.

Ali, S., Tang, X., Alavi, S. and Faubion, J., 2011. Structure and physical properties of starch/poly vinyl alcohol/sodium montmorillonite nanocomposite films. Journal of agricultural and food chemistry, 59(23), pp. 12384-12395.

Andresen, M., Johansson, L.S., Tanem, B.S. and Stenius, P., 2006. Properties and characterization of hydrophobized microfibrillated cellulose. Cellulose, 13, pp. 665-677.

Araki, J., Wada, M. and Kuga, S., 2011. Steric stabilization of a cellulose microcrystal suspension by poly(ethylene glycol) grafting. Langmuir, 17(1), pp. 21-27.

Ashori, A., Harun, J., Raverty, W. and Yusoff, M., 2006. Chemical and morphological characteristics of Malaysian cultivated kenaf (Hibiscus cannabinus) fiber. Polymer-Plastics Technology and Engineering, 45(1), pp. 131-134.

Aziz, S., Ansell, M., Clarke, S. and Panteny, S., 2005. Modified polyester resins for natural fiber composites. Compos Sci Technol, 65, pp. 525–535.

Azizi Samir, M.A.S., Alloin, F. and Dufresne, A., 2005. Review of recent research into cellulosic whiskers, their properties and their application in nanocomposite field. Biomacromolecules, 6, pp. 612-626.

Azwa, Z.N., Yousif. B.F., Manalo, A.C. and Karunasena, W., 2013. A review on the degradability of polymeric composites based on natural fibres. Mater Des, 47, pp. 424-442.

Batouli, S., Zhu, Y., Nar, M. and D'Souza, N., 2014. Environmental performance of kenaf-fiber reinforced polyurethane: a life cycle assessment approach. Journal of Cleaner Production, 66, pp. 164-173.

Bee, S., Ratnam, C., Sin, L., Tee, T., Hui, D., Kadhum, A., Rahmat, A. and Lau, J., 2014. Effects of electron beam irradiation on mechanical properties and nanostructural-morphology of montmorillonite added polyvinyl alcohol composite. Composites Part B: Engineering, 63, pp. 141-153.

Bhatnagar, A. and Sain, M., 2005. Processing of cellulose nanofiber-reinforced composites. Journal of Reinforced Plastics and Composites, 24(12), pp. 1259-1268.

Bledzki, A. and Gassan, J., 1999. Composites reinforced with cellulose based fibres. Progress in polymer science, 24(2), pp. 221-274.

Bolgar, M., Hubball, J., Groeger, J., and Meronek, S., 2008. Handbook for the chemical analysis of plastic and polymer additives. [e-book] Florida: CRC Press Taylor & Francis Group. Available at Google Books <books.google.com> [Accessed 2 August 2014]

Chang, J., Jang, T., Ihn, K., Lee, W. and Sur, G., 2003. Poly (vinyl alcohol) nanocomposites with different clays: pristine clays and organoclays. Journal of Applied Polymer Science, 90(12), pp. 3208-3214.

Chen, D., Lawton, D., Thompson, M. and Liu, Q., 2012. Biocomposites reinforced with cellulose nanocrystals derived from potato peel waste. Carbohydrate polymers, 90(1), pp. 709-716.

Chen, P., and Zhang, L., 2006. Interaction and properties of highly exfoliated soy protein/montmorillonite nanocomposites. Biomacromolecules, 7, pp. 1700-1706.

Chowdhury, M., Beg, M. and Khan, M., 2013. Biodegradability of Nanoparticle Modified Fiber Reinforced Polyester Resin Nanocomposite. Procedia Engineering, 68, pp. 431-438.

Darder, M., Colilla, M., and Ruiz-Hitzky, E., 2003. Biopolymer-clay nanocomposites based on chitosan intercalated in montmorillonite. Chemistry of Materials, 15, pp. 3774-3780.

de Souza Lima, M. and Borsali, R., 2004. Rodlike cellulose microcrystals: Structure, properties and applications. Macromol. Rapid Commun., 25, pp. 771-787.

Dean, K., Do, M., Petinakis, E. and Yu, L., 2008. Key interactions in biodegradable thermoplastic starch/poly (vinyl alcohol)/montmorillonite micro-and nanocomposites. Composites Science and Technology, 68(6), pp. 1453-1462.

Dhakal, H., Zhang. Z. and Richardson, M., 2007. Effect of water absorption on the mechanical properties of hemp fiber reinforced unsaturated polyester composites. Compos Sci Technol, 67, pp. 1674-83.

Dufresne, A., 2008. Cellulose-based composites and nanocomposites. Monomers, polymers and composites from renewable resources, pp. 401-418.

Dufresne, A. and Nalwa, H., 2011. Polymer nanocomposites from biological sources. Encyclopedia of Nanoscience and Nanotechnology, 219(250), pp. 32.

Ebina, T., and Mizukami, F., 2007. Flexible transparent clay films with heat-resistant and high gas-barrier properties. Advanced Materials, 19, pp. 2450–2453.

El-Shekeil, Y., Salit, M., Abdan, K. and Zainudin, E., 2011. Development of a new kenaf bast fiber-reinforced thermoplastic polyurethane composite. BioResources, 6(4), pp. 4662-4672.

El-Shekeil, Y., Sapuan, S., Jawaid, M. and Al-Shuja'a, O., 2014. Influence of fiber content on mechanical, morphological and thermal properties of kenaf fibers reinforced poly (vinyl chloride)/thermoplastic polyurethane poly-blend composites. Materials & Design, 58, pp. 130-135.

Faruk, O., Bledzki, A., Fink, H. and Sain, M., 2012. Biocomposites reinforced with natural fibers: 2000-2010. Progress in Polymer Science, 37(11), pp. 1552-1596.

Fortunati, E., Luzi, F., Puglia, D., Dominici, F., Santulli, C., Kenny, J. and Torre, L., 2014. Investigation of thermo-mechanical, chemical and degradative properties of PLA-limonene films reinforced with cellulose nanocrystals extracted from Phormium tenax leaves. European Polymer Journal, 56, pp. 77-91.

Fortunati, E., Puglia, D., Luzi, F., Santulli, C., Kenny, J. and Torre, L., 2013. Binary PVA bio-nanocomposites containing cellulose nanocrystals extracted from different natural sources: Part I. Carbohydrate polymers, 97(2), pp. 825-836.

Frone, A., Panaitescu, D. and Donescu, D., 2011. Some aspects concerning the isolation of cellulose micro-and nano-fibers. UPB Buletin Stiintific, Series B: Chemistry and Materials Science, 73(2), pp. 133-152.

Gad, Y.H., 2009. Improving the properties of poly(ethylene-co-vinyl acetate)/clay composite by using electron beam irradiation. Nucl Instrum Meth Phys Res B, 267, pp. 3528-34.

George, J., Sreekala, M. and Thomas, S., 2011. A review on interface modification and characterization of natural fiber reinforced plastic composites. Polym Eng Sci, 41, pp. 1471-1485.

Graupner, N., R"ossler, J., Ziegmann, G. and M"ussig, J., 2014. Fibre/matrix adhesion of cellulose fibres in PLA, PP and MAPP: A critical review of pull-out test, microbond test and single fibre fragmentation test results. Composites Part A: Applied Science and Manufacturing, 63, pp. 133-148.

Grossman, R., and Lutz, J., 2001. Polymer Modifiers and Additives. [e-book] New York: Marcel Dekker, Inc. Available at Google Books <books.google.com> [Accessed 2 August 2014]

Guirguis, O. and Moselhey, M., 2011. Thermal and structural studies of poly (vinyl alcohol) and hydroxypropyl cellulose blends. Scientific Research Publishing, 4, pp. 57-67.

Han, S., Karevan, M., Sim, I., Bhuiyan, M., Jang, Y., Ghaffar, J., and Kalaitzidou, K., 2012. Understanding the ReinforcingMechanisms in Kenaf Fiber/PLA and Kenaf Fiber/PP Composites: A Comparative Study. International Journal of Polymer Science, pp. 1-8.

Hassan, C. and Peppas, N., 2000. Structure and applications of poly(vinyl alcohol) hydrogels produced by conventional crosslinking or by freezing/thawing methods. Advances in Polymer Science, 153, pp. 38-62.

He, H., Zhu, J., Yuan, P., Zhou, Q., Ma, Y. and Frost, R., 2008. Pore structure of surfactant modified montmorillonites. Australasian Institute of Mining and Metallurgy Publications, 8, pp. 321-327.

Helbert, W., Cavaille, J. and Dufresne, A., 1996. Thermoplastic nanocomposites filled with wheat straw cellulose whiskers. Part I: processing and mechanical behavior. Polymer composites, 17(4), pp. 604-611.

Hietala, M., Mathew, A. and Oksman, K., 2013. Bionanocomposites of thermoplastic starch and cellulose nanofibers manufactured using twin-screw extrusion. European Polymer Journal, 49(4), pp. 950-956.

Jia, X., Li, Y., Cheng, Q., Zhang, S. and Zhang, B., 2007. Preparation and properties of poly (vinyl alcohol)/silica nanocomposites derived from copolymerization of vinyl silica nanoparticles and vinyl acetate. European polymer journal, 43(4), pp. 1123-1131.

Jo, B., Park, S. and Kim, D., 2008. Mechanical properties of nano-MMT reinforced polymer composite and polymer concrete. Construction and building Materials, 22(1), pp. 14-20.

Johansson, C., Bras, J., Mondragon, I., Nechita, P., Plackett, D., Simon, P., and others., 2012. Renewable fibers and bio-based materials for packaging applications - a review of recent developments. BioResources, 7, pp. 2506-2552.

John, M. and Thomas, S., 2008. Biofibres and biocomposites. Carbohydrate polymers, 71(3), pp. 343-364.

Kargarzadeh, H., Ahmad, I., Abdullah, I., Dufresne, A., Zainudin, S. Y. and Sheltami, R. M., 2012. Effect of hydrolysis conditions on the morphology, crystallinity, and

thermal stability of cellulose nanocrystals extracted from kenaf bast fibers. Cellulose, 19, pp. 855-866.

Khalina, A., Jalaluddin, H. and Yeong, H., n.d. Properties of kenaf (Hibiscus Cannabinus L.) Bast fibre reinforced unsaturated polyester composite. In: Research in Natural fibre reinforced polymer composites. pp. 233-246.

Kim, W., Argento, A., Lee, E., Flanigan, C., Houston. D., Harris, A. and others, 2012. High strain-rate behavior of natural fiber-reinforced polymer composites. J Compos Mater, 46, pp. 1051-65.

Kowalczyk, M., Piorkowska, E., Kulpinski, P. and Pracella, M., 2011. Mechanical and thermal properties of PLA composites with cellulose nanofibers and standard size fibers. Composites Part A: Applied Science and Manufacturing, 42(10), pp. 1509-1514.

Lakshmi, M., Narmadha, B. and Reddy, B., 2008. Enhanced thermal stability and structural characteristics of different MMT-clay/epoxy-nanocomposite materials. Polymer Degradation and Stability, 93(1), pp. 201-213.

Lee, S., Mohan, D., Kang, I., Doh, G., Lee, S. and Han, S., 2009. Nanocellulose reinforced PVA composite films: effects of acid treatment and filler loading. Fibers and Polymers, 10(1), pp. 77-82.

Lee, T., Bee, S., Tee, T., Kadhum, A.A.H., Ma, C., Rahmat, A.R. and Veerasamy, P., 2013. Characterization of α-tocopherol as interacting agent in polyvinyl alcohol-starch blends. Carbohydrate Polymers, 98, pp. 1281-1287.

Lee, T., Rahman, W., Rahmat, A. and Khan, M., 2010. Detection of synergistic interactions of polyvinyl alcohol–cassava starch blends through DSC. Carbohydrate Polymers, 79(1), pp.224-226.

Lenza, J., Merkel, K. and Rydarowski, H., 2012. Comparison of the effect of montmorillonite, magnesium hydroxide and a mixture of both on the flammability properties and mechanism of char formation of HDPE composites. Polymer Degradation and Stability, 97(12), pp. 2581-2593.

Li, D. and Sur, G.S., 2014. Comparison of poly(ethylene-co-acrylic acid) loaded Zn2+-montmorillonite nanocomposites and poly(ethylene-co-acrylic acid) zinc salt. Journal of Industiral and Engineering Chemistry, 20, pp. 3122-3127.

Li, W., Wu, Q., Zhao, X., Huang, Z., Cao, J. and Liu, S., 2014. Enhanced thermal and mechanical properties of PVA compositesformed with filamentous nanocellulose fibrils. Carbohydrate Polymers, 113, pp. 403-410.

Li, X., Tabil, L. and Panigrahi, S., 2007. Chemical treatments of natural fiber for use in natural fiber-reinforced composites: a review. Journal of Polymers and the Environment, 15(1), pp. 25-33.

Liu, G., Song, Y., Wang, J., Zhuang, H., Ma, L., Li, C., Liu, Y. and Zhang, J., 2014. Effects of nanoclay type on the physical and antimicrobial properties of PVOH-based nanocomposite films. LWT-Food Science and Technology, 57(2), pp. 562-568.

Majdzadeh-Ardakani, K. and Nazari, B., 2010. Improving the mechanical properties of thermoplastic starch/poly (vinyl alcohol)/clay nanocomposites. Composites Science and Technology, 70(10), pp. 1557-1563.

Majeed, K., Jawaid, M., Hassan, A., Abu Bakar, A., Abdul Khalil, H., Salema, A. and Inuwa, I., 2013. Potential materials for food packaging from nanoclay/natural fibres filled hybrid composites. Materials & Design, 46, pp. 391-410.

Mandal, A. and Chakrabarty, D., 2014. Studies on the mechanical, thermal, morphological and barrier properties of nanocomposites based on poly (vinyl alcohol) and nanocellulose from sugarcane bagasse. Journal of Industrial and Engineering Chemistry, 20(2), pp. 462-473.

Murphy, J., 2001. Additives for Plastics Handbook. [e-book] Oxford: Elsevier Science Ltd. Available at Google Books <books.google.com> [Accessed 2 August 2014]

Ning, N., Fu, S., Zhang, W., Chen, F., Wang, K., Deng, H., Zhang, Q. and Fu, Q., 2012. Realizing the enhancement of interfacial interaction in semicrystalline polymer/filler composites via interfacial crystallization. Progress in Polymer Science, 37(10), pp. 1425-1455.

Nishino, T., Hirao, K., Kotera, M., Nakamae, K. and Inagaki, H., 2003. Kenaf reinforced biodegradable composite. Composites Science and Technology, 63(9), pp. 1281-1286.

Nishino, T., Hirao, K. and Kotera, M., 2006. X-ray diffraction studies on stress transfer of kenaf reinforced poly (l-lactic acid) composite. Composites Part A, 37(12), pp. 2269-2273.

Ochi, S., 2008. Mechanical properties of kenaf fibers and kenaf/PLA composites. Mechanics of materials, 40(4), pp. 446-452.

Olabisi, O., 1997. Handbook of Thermoplastics. [e-book] New York: Marcel Dekker, Inc. Available at Google Books <books.google.com> [Accessed 2 August 2014]

Özturk, S., 2010. Effect of fiber loading on the mechanical properties of kenaf and fiberfrax fiber-reinforced phenol-formaldehyde composites. J Comp Mater, 44, pp. 2265.

Paul, D.R., 2008. Robeson LM. Polymer nanotechnology: nanocomposites. Polymer, 49, pp. 3187-204.

Pereira, A., Nascimento, D., Morais, J., Vasconcelos, N., Feitosa, J., Br'igida, A., Rosa, M. and others, 2014. Improvement of polyvinyl alcohol properties by adding nanocrystalline cellulose isolated from banana pseudostems. Carbohydrate Polymers, 112, pp. 165-172.

Qiu, K. and Netravali, A., 2012. Fabrication and characterization of biodegradable composites based on microfibrillated cellulose and polyvinyl alcohol. Composites Science and Technology, 72(13), pp. 1588-1594.

Rahmat, A., Rahman, W., Sin, L. and Yussuf, A., 2009. Approaches to improve compatibility of starch filled polymer system: A review. Materials Science and Engineering: C, 29(8), pp. 2370-2377.

Reddy, M., Vivekanandhan, S., Misra, M., Bhatia, S. and Mohanty, A., 2013. Biobased plastics and bionanocomposites: Current status and future opportunities. Progress in Polymer Science, 38(10), pp. 1653-1689.

Reho, G., 2012. *Characterisation of montmorillonite on polyvinyl alcohol-starch compound*. Degree of Bachelor. Universiti Tunku Abdul Rahman.

Rwei, S.P. and Huang, C. C., 2012. Electrospinning PVA solution-rheology and morphology analysis. Fibers Polym, 13 (1), pp. 44-50.

Santa Clara University Engineering Design Centre, n.d. Additives, fillers and reinforcements. [online] Available at: <http://www.dc.engr.scu.edu/cmdoc/dg_doc/develop/material/overview/a3000002.htm> [Accessed 3 August 2014].

Schulz, M., Kelkar, A., and Sundaresan, M., 2006. Nanoengineering of Structural, Functional and Smart Materials. [e-book] Florida: CRC Press Taylor & Francis Group. Available at: Google Books <books.google.com> [Accessed 12 August 2014].

Shi, J., Shi, S., Barnes, H., Pittman Jr, C. and others, 2011. A chemical process for preparing cellulosic fibers hierarchically from kenaf bast fibers. BioResources, 6(1), pp. 879-890.

Silv'erio, H., Flauzino Neto, W., Dantas, N. and Pasquini, D., 2013. Extraction and characterization of cellulose nanocrystals from corncob for application as

reinforcing agent in nanocomposites. Industrial Crops and Products, 44, pp. 427-436.

Siqueira, G., Bras, J. and Dufresne, A., 2010. Cellulosic bionanocomposites: a review of preparation, properties and applications. Polymers, 2(4), pp. 728-765.

Strawhecker, K. and Manias, E., 2000. Structure and properties of poly(vinyl alcohol)/Na+ montmorillonite nanocomposites. Chem. Mater., 12 (10), pp. 2943-2949.

Taghizadeh, M. T. and Sabouri, N., 2013. Study of enzymatic degradation and water absorption of nanocomposites polyvinyl alcohol/starch/carboxymethyl cellulose blends containing sodium montmorillonite clay nanoparticle by cellulase and α-amylase. Journal of the Taiwan Institute of Chemical Engineers, 44, pp. 995-1001.

Tang, X. and Alavi, S., 2011. Recent advances in starch, polyvinyl alcohol based polymer blends, nanocomposites and their biodegradability. Carbohydrate polymers, 85(1), pp. 7-16.

Tanpichai, S., Sampson, W. and Eichhorn, S., 2014. Stress Transfer in Microfibrillated Cellulose Reinforced Poly (vinyl alcohol) Composites. Composites Part A: Applied Science and Manufacturing, 65, pp. 186-191.

Tee, T., Sin, L., Gobinath, R., Bee, S., Hui, D., Rahmat, A., Kong, I. and Fang, Q., 2013. Investigation of nano-size montmorillonite on enhancing polyvinyl alcohol-starch blends prepared via solution cast approach. Composites Part B: Engineering, 47, pp. 238-247.

Thakur, V. and Thakur, M., 2014. Processing and characterization of natural cellulose fibers/thermoset polymer composites. Carbohydrate polymers, 109, pp. 102-117.

Tuncc, S. and Duman, O., 2010. Preparation and characterization of biodegradable methyl cellulose/montmorillonite nanocomposite films. Applied Clay Science, 48(3), pp. 414-424.

Ul-Islam, M., Khan, T. and Park, J., 2012. Nanoreinforced bacterial cellulose-montmorillonite composites for biomedical applications. Carbohydrate polymers, 89(4), pp. 1189-1197.

Velmurugan, R. and Mohan, T., 2004. Room temperature processing of epoxy-clay nanocomposites. Journal of Materials Science, 39(24), pp.7333-7339.

Visakh, P., Thomas, S., Chandra, A. and Mathew, A., 2013. Advances in elastomers II: composites and nanocomposites. [e-book] New York: Springer-Verlag Berlin Heidelberg. Available at Google Books <books.google.com> [Accessed 2 August 2014]

Wambua, P., Ivens, J. and Verpoest I., 2003. Natural fibers: can they replace glass in fiber reinforced plastics? Compos Sci Technol, 63, pp. 1259-1264.

Wang, T., 2011. Cellulose nanowhiskers and nanofibers from biomass for composite applications. PhD. Michigan State University.

Whelan, T., 1994. Polymer Technology Dictionary. [e-book] London: Chapman & Hall. Available at Google Books <books.google.com> [Accessed 2 August 2014]

Yang, Q., Wu, C., Saito, T. and Isogai, A., 2014. Cellulose--clay layered nanocomposite films fabricated from aqueous cellulose/LiOH/urea solution. Carbohydrate polymers, 100, pp. 179-184.

Yiu, W., and Zhong, Z., 2006. Polymer nanocomposites. [e-book] Florida: Woodhead Publishing Limited. Available at Google Books <books.google.com> [Accessed 2 August 2014]

Zaaba, N., Ismail, H. and Jaafar, M., 2014. The Effects of Modifying Peanut Shell Powder with Polyvinyl Alcohol on the Properties of Recycled Polypropylene and Peanut Shell Powder Composites. BioResources, 9(2), pp. 2128-2142.

Zaini, L., Jonoobi, M., Tahir, P. and Karimi, S., 2013. Isolation and characterization of cellulose whiskers from kenaf (Hibiscus cannabinus L.) bast fibers. Journal of Biomaterials and Nanobiotechnology, 4, p. 37.

Zainuddin, S., Ahmad, I., Kargarzadeh, H., Abdullah, I. and Dufresne, A., 2013. Potential of using multiscale kenaf fibers as reinforcing filler in cassava starch-kenaf biocomposites. Carbohydrate polymers, 92(2), pp. 2299-2305.